70-22,991

JONES, Robert Warner, 1932-
ACCELERATION OF HURRICANE BETSY ON 29 AUGUST 1965.

The University of Oklahoma, Ph.D., 1970
Physics, meteorology

University Microfilms, A XEROX Company, Ann Arbor, Michigan

THE UNIVERSITY OF OKLAHOMA

GRADUATE COLLEGE

ACCELERATION OF HURRICANE BETSY

ON 29 AUGUST 1965

A DISSERTATION

SUBMITTED TO THE GRADUATE FACULTY

in partial fulfillment of the requirements of

the degree of

DOCTOR OF PHILOSOPHY

By

ROBERT WARNER JONES

Norman, Oklahoma

1970

ACCELERATION OF HURRICANE BETSY

ON 29 AUGUST 1965

APPROVED BY

Robert M. St. John

W J Saucier

DISSERTATION COMMITTEE

ACKNOWLEDGEMENTS

The writer expresses his appreciation to Professor Yoshikazu Sasaki who sponsored this research and whose comments on the manuscript were most helpful. The Oklahoma University computer center granted ten hours of free computer time to perform numerical computations. The research was supported by the National Science Foundation through a grant to the University of Oklahoma. The manuscript was typed by Jan Stone and Marcia Rucker. Figures were drafted by Droescher and Associates.

TABLE OF CONTENTS

LIST OF TABLES

LIST OF ILLUSTRATIONS

ABSTRACT

The acceleration of Hurricane Betsy 1965, which was observed to decrease its speed from 12 to 6 kts between 1600 and 2110 GMT on 29 August while moving in a mean direction toward 330 degrees, is studied by use of reconnaissance aircraft data at 11,780 feet, collected by the National Hurricane Research Laboratory, and from synoptic data. These data reveal an inside and outside of the storm where the basic current, defined to be uniform over the region in which it is determined, disagrees and agrees, respectively, with the environment steering current. The basic current observed by reconnaissance aircraft over a 125 km disk is 287° 2.7 kt and the steering current at 700 mb at 1200 GMT is near 120° 15 kt.

The acceleration of Betsy, viewed from the outside, is discussed with the aid of Kuo's model of storm-environment interaction, including eddy viscosity, and is extended to a time changing steering current. The storm's velocity and mean acceleration vectors are predicted to be to the right of the corresponding steering current vectors. The environment data, which are scarce, appear to confirm this.

The acceleration of Betsy, viewed from the inside, is examined with the reconnaissance aircraft data. The important observations are the basic current cited above and an unbalanced uniform gradient of the geopotential (pressure), which is colinear with the observed mean storm acceleration but about five times larger in magnitude. This force is

probably the manifestation, inside the storm, of the storm-environment interaction, taking place outside 125 km. To explain the storm acceleration in terms of this force, an adjustment mechanism depending on the storm rotation is hypothesized. The mean acceleration of air parcels down the geopotential gradient may occur at the storm acceleration rate while instantaneous parcel accelerations may occur at a rate corresponding to the unbalanced force. The parameter $f/(f+\bar{Z})$ is introduced to connect the acceleration scales where f is the Coriolis parameter and $\bar{Z}$ is the mean angular speed of the storm core. The parameter is .22 and the empirical relation between the mean storm acceleration and the unbalanced force is .18. This mechanism should generate gravity-inertia oscillations of period near six hours and may generate a basic current directed down the geopotential gradient. Both conditions are observed in the wind data.

The acceleration of the wind in the coordinate moving with the storm center was examined with the result that the wind acceleration is primarily an adjustment toward balance with the symmetric geopotential which shows a deepening trend in these data.

ACCELERATION OF HURRICANE BETSY ON 29 AUGUST 1965

CHAPTER I

INTRODUCTION

Prediction of the track of the hurricane or typhoon is one of the most challenging problems in meteorology. By tracking the storm by meteorological satellite and by aircraft, the past track and current position and velocity of the storm are known at the time a forecast is to be made. The essential difficulty is to be able to anticipate changes in the velocity of the storm or departures from persistence of the present velocity. Fortunately, the hurricane tends to persist in its current state of motion which gives the forecaster an important tool, but this state can be changed by exerting a net force to accelerate the storm.

The most difficult part of the hurricane acceleration problem is the lack of adequate data. To understand this, note that a measure of the size or scale of the hurricane is the diameter of the maximum wind belt which is of the order of 100 km. The average distance between tropcal observation stations, which collect data to give the three-dimensional structure of the atmosphere, is much larger than this so that the hurricane cannot be described by these data. This circumstance has limited progress in understanding and forecasting the movement of the hurricane and has caused primary emphasis to be placed upon describing and forecasting the environment air currents in which the hurricane is embedded.

The scale of the environment current is about 1000 km and more success is possible in this endeavor. Then, if the hurricane motion is related to its environment, some success is possible in forecasting its motion. To emphasize the role of the environment flow patterns, commonly referred to as the steering current, is logical because the movement of a hurricane is essentially a question of the interaction between the storm and its environment, and all studies of hurricane motion have found the major influence to be that of the environment.

The acceleration of the hurricane is controlled by a set of thermo-hydrodynamic equations which apply to the atmosphere. To get at the essential mechanisms of acceleration, simplified models of the movement of the hurricane have been devised. Two types of models may be of interest, the steering models and the hydrodynamic models, and both types give prime importance to the environment steering current. The difference between these models is that the interaction between the hurricane and its environment is idealized to occur at and outside a radius R in the hydrodynamic models but occurs over the whole storm in the steering models.

The steering principle, which assumes that the hurricane moves with a suitably defined and predicted steering current, is a well known and useful tool of tropical weather forecasters and is discussed in the book by Riehl (1954). This principle was first formulated in a dynamical model for numerical prediction by digital computer by Sasaki and Miyakoda (1954). They assumed a barotropic atmosphere and, after removing the hurricane vortex from the data to determine the steering current, they forecast this current with the barotropic vorticity equation. The hurricane is assumed to be symmetric and follows the predicted steering current with a westward drift added to account for the variation of the Coriolis parameter. Since their paper, many others have followed this approach adding various details to the computations. Some success is reported and steering models are used for operational numerical prediction of hurricane tracks. The advantage of the steering model is that it does not require detailed observations of the wind and pressure fields of the hurricane in order to be able to execute a forecast, but it does rely upon data appropriate to describe the environment flow.

The hydrodynamic models follow an approach similar to the classical hydrodynamic treatment of a cylinder moving in a two-dimensional fluid. The acceleration of the cylinder or hurricane is controlled by the Coriolis, drag, and pressure forces acting upon it. The pressure distribution about the storm is computed from a model of the wind field which takes account of the steering current and the structure of the storm.

Classical hydrodynamics was applied to the hurricane acceleration problem by Yeh (1950). Yeh's paper assumes a two-dimensional, incompressible and homogeneous fluid for the environment steering current and concludes that the storm followed the steering current, which was uniform, but also with an oscillation due to the rotation of the storm superposed to give a trochoidal path. Kuo (1969) added eddy viscosity as drag forces upon the cylinder and environment to show that the mean path of the storm may deviate from the steering current. The deviation is to the right of the steering current for a cyclonic vortex, and the motion follows a damped trochoidal path about the mean path, which is straight in a uniform steering current. Sasaki and Syono (1968) have included non-symmetric winds of the vortex. By filtering out the oscillation in the path, due to the Kutta-Joukowski or rotor force which appears in Yeh's and Kuo's models, an equation for the hurricane acceleration is obtained which allows air to flow across the cylinder boundary. These models will be discussed in more detail in Chapter VI. They are two-dimensional and are so because the tropical steering current tends to be barotropic, but important consequences of three-dimensional motion of the atmosphere may be missing. Also, the radius where the storm-environment interaction occurs is not given by the theory, but must be determined experimentally.

Very little data have been published relating the structure of the hurricane to its movement. It is the purpose of this paper to take advantage of aircraft data collected by the National Hurricane Research Laboratory (NHRL) of the Environmental Sciences Services Administration (ESSA) at Miami, Florida, to describe to the extent possible, using one level of data, the relation between the storm structure, its environment and its motion. Use of a single data level restricts the results to be obtained. It is done mostly for convenience. The selected case proves interesting, but only one data level was available. Data were selected for Hurricane Betsy on 29 August 1965. The reference level of the data is 11,780 feet. The data were collected between 1530 and 2330 GMT from the center of the storm out to 125 km radius. This case was selected because a significant acceleration of the storm was observed during the data collection and the data coverage out to 125 km was good. At this time, Betsy was classified as a tropical storm, which has a structure similar to the hurricane but the maximum wind speed is between 39 and 73 mi hr^{-1} rather than in excess of 74 mi hr^{-1}. The maximum wind was 65 mi hr^{-1}.

The mean velocity of Betsy varies from 300° 12 kt to 300° 6 kt between 1600 and 2110 GMT. The environment steering current is estimated from 700 mb, about 10,000 feet, to be 120° 15 kt at 1200 GMT and 110° 8 kt at 2400 GMT on 29 August 1965. Analysis of the aircraft wind data reveals a uniform current, referred to as the basic current, measured over a disk of 125 km radius which is 287° 2.7 kt. It is customary to refer to the direction toward which a storm moves, but from which a wind blows. North is 0 or 360 degrees, east is 90 degrees, and so forth. Later, a polar coordinate system will be introduced with the appropriate mathematical conventions.

These data reveal that the basic current inside the storm differs completely from the motion of the storm and from the environment steering current so that the steering principle does not hold in its usual form. Also, the interaction between the storm and the environment, discussed by Yeh, Kuo, or Sasaki and Syono, must occur at a radius greater than 125 km. The data reveal an inside and an outside of the storm where the basic current may disagree and agree, respectively, with the environment.

On the outside, the storm is moving about 30 degrees to the right of the 700 mb current. Wind data at other levels in the environment suggest that the 700 mb wind may be typical of the wind in a layer from the ocean surface to 15,000 feet. This deviation of the storm motion from the steering current agrees with Kuo's result for a cyclonic vortex. The storm acceleration vector is also nearly 30 degrees to the right of the steering current acceleration vector. By extending Kuo's results to a time variable steering current, it is shown in Chapter VI that the latter observation follows also.

Discussion of the acceleration of Betsy, viewed from the aircraft data within 125 km, is difficult because no previous theory applies here. To begin examination of this question, a two-dimensional model of the wind and geopotential is given in Chapter II following Sasaki and Syono. After a discussion of the analysis of the aircraft data and computation of the basic current in Chapter III, this model is used to discuss the balance of wind and geopotential at 11,780 feet in Chapter IV. An unbalanced uniform geopotential gradient force is found which is colinear with the storm acceleration, but is about five times greater in magnitude. Much of Chapters V and VI are concerned with interpretation of this force.

The wind acceleration, observed by the aircraft at points where the flight path intersects itself in a coordinate system moving with the center of the storm, is discussed in Chapter V. The wind appears to be approaching gradient equilibrium and not much influenced by the unbalanced linear geopotential force. This result shows a dominance of the symmetric over the non-symmetric geopotential.

In Chapter VI a hypothesis is presented relating the unbalanced linear geopotential force to the acceleration of the storm. It is hypothesized that the storm acceleration is colinear with the geopotential force but reduced by the factor $f/(f + \overline{Z})$ where f is the Coriolis parameter and $\overline{Z}$ is the area mean angular velocity of the storm within 125 km radius. The mechanism of the storm acceleration is an adjustment problem controlled by the Coriolis, centrifugal, and pressure forces. The parameter $f/(f + \overline{Z})$ is chosen because the current oscillation of adjustment is controlled by $f + Z$ rather than f, as is the case when no rotation in the wind occurs. The observed value of $f/(f + \overline{Z})$ is .22, which agrees with the results of Chapter IV. This is a hypothesis and theoretical justification remains to be done. The origin of the unbalanced geopotential force is hypothesized to be the result of interaction between the environment and the storm. This is discussed from the viewpoint of Kuo's model extended to include a time variable steering current. The problem of the steering or movement of the interior of Betsy toward 300 degrees is discussed and the conclusion is that the storm vorticity field may be moved by the observed wind field rather than by just the basic current. The observed wind speed is greater on the right than on the left side of the storm looking in the direction of motion. This is the basis of the conclusion. The role of vertical momentum transports and convection in the motion of the storm interior is briefly discussed.

Following Chapter VI is a brief discussion and summary of results obtained.

CHAPTER II

MODEL OF ASYMMETRIC HURRICANE

Basic Equations

A simple model of a two-dimensional non-symmetric hurricane has been investigated by Sasaki and Syono (1966). The essential concept of this model is to describe the interaction between the hurricane vortex and its environment. The environment is introduced through the environment steering current, which is a uniform stream with constant shear superposed. The symmetric circulation of the hurricane is represented by the singular vortex located at the storm center and the non-symmetric vortex flow is given by a doublet, which may be regarded as either the superposition of two singular vortices of opposite sign or as a singular source-sink pair. The doublet may approximate asymmetry due to pure rotational or divergent motion or a combination of both, provided the axes between the vorticity and divergence centers are perpendicular. By use of the hydrodynamic equations for two-dimensional motion, the corresponding pressure or geopotential solutions are obtained as simple analytic functions.

The domain or region in which the model describes the wind and pressure is bounded by infinity and by a circle of radius R surrounding the storm center. This region is primarily the environment of the storm, although R must be inside the storm circulation. The wind fields chosen to approximate the hurricane are intended to give the influence of the hurricane upon the environment without having to consider the details of the motion inside R. The wind fields of the hurricane are determined by giving the wind at R and the environment winds are specified by the boundary condition as r, the distance from the vortex center, approaches infinity. It may be noted that the domain in which the reconnaissance flight data are gathered corresponds more to the region inside R than outside so that there may be some difficulty fitting this data to the model. But since the value of R, where this model may apply, is not known in advance, the data are worth examining from the viewpoint of the model.

The two-dimensional assumption is based upon the reasonable expectation that, because the large-scale synoptic wind fields of the subtropics where hurricanes occur are often nearly barotropic or two-dimensional above the boundary layer, the essential mechanism of interaction of hurricane and environment may be approached in this way. The boundary layer is the transition region between the earth's surface, where the viscous boundary condition requires the velocity to vanish, and the free atmosphere. It is fully turbulent and dominated by eddy viscosity. Kuo (1969) shows the importance of eddy viscosity in the boundary layer upon the motion of a vortex.

The equations appropriate for discussion of the wind and pressure fields of a moving hurricane are the Eulerian equations of hydrodynamics, written for a horizontal moving coordinate (x_i), with center X_i coinciding with the hurricane center. With restriction to two-dimensional homogeneous incompressible flow, but including eddy viscosity in the boundary layer, the equations may be written

$$\frac{\partial u_i}{\partial t} + \ddot{X}_i + u_j \frac{\partial u_i}{\partial x_j} - \epsilon_{ijk}\Omega_k (u_j + \dot{X}_j) = - \frac{\partial \varphi}{\partial x_i} + \mu (u_i + \dot{X}_i) \tag{2.1}$$

and

$$\frac{\partial u_i}{\partial x_i} = 0 \tag{2.2}$$

where i and j are 1 or 2 and k is taken as 1, 2, or 3; u_i is the i-th component of the velocity in the moving coordinate; and φ is the geopotential which equals p/ρ where p is the pressure and ρ the density of the fluid. The coefficient ϵ_{ijk} is the alternating third order tensor and Ω_k has components (0, 0, f) where f is the Coriolis parameter.

The term $\mu(u_i + \dot{X}_i)$ is the surface stress per unit mass for a layer of unit thickness and is similar to the stress introduced by Kuo in the environment except that here the stress is proportional to the wind measured in the fixed rather than the relative coordinate. The coefficient μ may be referred to as a friction coefficient. In general, μ is a function of the wind speed and this is important when considering the strong symmetric winds of the hurricane. But the analysis below shows that where the symmetric wind is multiplied by μ, this term does not influence the geopotential but enters a separate vorticity equation for the symmetric circulation. Since μ influences the asymmetric geopotential only through the steering current and doublet flow, which are small compared to the symmetric wind, it is reasonable to take μ constant here. The influence of the symmetric wind drag on the motion of the hurricane is introduced in the discussion in Chapter VI, where it is important. Persuant to addition of friction to this discussion, it is necessary to consider time variations of the symmetric wind of the vortex and vorticity of the steering current. And to complete the discussion of the symmetric circulation Γ, a source of strength m is introduced at the origin of the moving coordinate.

The boundary conditions required to solve (2.1) and (2.2) are that φ and v_n, the normal velocity to the boundary, be known on the boundaries or

$$\varphi \text{ and } v_n \text{ given on the boundaries.} \tag{2.3}$$

The boundaries which are convenient for the hurricane problem are, at $r = R$ and infinity, as noted above.

The non-divergent condition (2.2) implies a diagnostic relation between wind and geopotential which is obtained by applying the divergence operator to (2.1). The result is known as the balance equation and is

$$\frac{\partial}{\partial x_i} \frac{\partial}{\partial x_i} \varphi = - \frac{\partial}{\partial x_j} u_i \frac{\partial}{\partial x_i} u_j + \epsilon_{ijk} \frac{\partial}{\partial x_i} (u_j \Omega_k) . \tag{2.4}$$

The hurricane model is a set of equations relating wind and geopotential at a given instant of time and is obtained from (2.4). The model is obtained by assuming the wind field and computing geopotential from (2.4).

Note that this is far easier than assuming geopotential and computing the wind as (2.4), as well as (2.1), is non-linear in the wind but linear in the geopotential.

The procedure for constructing the model is to specify the wind field which is represented by the streamfunction for non-divergent flow. The streamfunction satisfies a Poisson equation and v_n is given on the boundary to complete the solution. Then, (2.4) is solved for φ using the streamfunction for the right hand side. From this viewpoint, (2.4) is a Poisson equation and requires φ on the boundary to obtain the solution of the homogeneous equation. This part of the solution is obtained from (2.1) by inserting the wind on the left hand side, after transposing the friction term, including time changes of the wind and solving for φ. The solution of the Poisson equation is given on a polar coordinate with the origin at the hurricane center. The entire φ solutions may be obtained from (2.1) without (2.4), similar to forming the Bernoulli equation. The procedure outlined here may appear to be inconsistent with (2.3) for (2.1) is used to compute boundary values of φ; but, in doing so, (2.1) is being used as a diagnostic rather than a prognostic equation because the time change of the wind is assumed.

Wind Field

The non-divergent condition (2.2) allows the streamfunction ψ to be introduced to represent the wind field. The streamfunction at a particular instant of time in the moving coordinate (moving with the velocity components $\dot{X}$ and $\dot{Y}$) is the solution of

$$\nabla^2\psi = \zeta \tag{2.5}$$

where ζ is the vorticity of the fluid which is uniform in space. If the circulation of the hurricane is Γ and the strength of the source is m, the solution of (2.5), assuming circular geometry and subject to boundary conditions given below, is

$$\psi = \frac{\zeta}{4}[(X+r\cos\theta)^2+(Y+r\sin\theta)^2] + \frac{\Gamma}{2\pi}\ln r - \frac{m}{2\pi}\theta$$
$$+\sum_{n=1}^{\infty}[(\Psi_n r^n + \Psi_{-n} r^{-n})\cos n\theta + (\Psi_n^* r^n + \Psi_{-n}^* r^{-n})\sin n\theta] \tag{2.6}$$

where X, Y, Γ, m, ζ, Ψ_n, Ψ_{-n}, Ψ_n^* and Ψ_{-n}^* are functions of time only.

The x and y components of the velocity in the moving coordinates are u and v and are given by

$$u = -\frac{\partial\psi}{\partial y} = -\frac{\zeta}{2}(Y+r\sin\theta) - \frac{\Gamma}{2\pi r}\sin\theta + \frac{m}{2\pi r}\cos\theta$$
$$+\sum_{n=1}^{\infty}[n\Psi_n r^{n-1}\sin(n-1)\theta + n\Psi_{-n} r^{-n-1}\sin(n+1)\theta \tag{2.7}$$
$$- n\Psi_n^* r^{n-1}\cos(n-1)\theta - n\Psi_{-n}^* r^{-n-1}\cos(n+1)\theta],$$

$$v = \frac{\partial\psi}{\partial x} = \frac{\zeta}{2}(X + r\cos\theta) + \frac{\Gamma}{2\pi r}\cos\theta + \frac{m}{2\pi r}\sin\theta$$

$$+ \sum_{n=1}^{\infty} [n\Psi_n r^{n-1}\cos(n-1)\theta - n\Psi_{-n} r^{-n-1}\cos(n+1)\theta \tag{2.8}$$

$$+ n\Psi_n^* r^{n-1}\sin(n-1)\theta - n\Psi_{-n}^* r^{-n-1}\sin(n+1)\theta] .$$

The radial and tangential velocity components are v_r and v_θ and are given by

$$v_r = -\frac{1}{r}\frac{\partial\psi}{\partial\theta} = \frac{\zeta}{2}(X\sin\theta - Y\cos\theta) + \frac{m}{2\pi r}$$

$$+ \sum_{n=1}^{\infty} [n(\Psi_n r^{n-1} + \Psi_{-n} r^{-n-1})\sin n\theta \tag{2.9}$$

$$- n(\Psi_n^* r^{n-1} + \Psi_{-n}^* r^{-n-1})\cos n\theta]$$

and

$$v_\theta = \frac{\partial\psi}{\partial r} = \frac{\zeta}{2}(X\cos\theta + Y\sin\theta + r) + \frac{\Gamma}{2\pi r}$$

$$+ \sum_{n=1}^{\infty} [n(\Psi_n r^{n-1} - \Psi_{-n} r^{-n-1})\cos n\theta \tag{2.10}$$

$$+ n(\Psi_n^* r^{n-1} - \Psi_{-n}^* r^{-n-1})\sin n\theta] .$$

The coefficients Ψ_n, Ψ_{-n}, Ψ_n^* and Ψ_{-n}^* must be determined by specifying the velocity on the boundaries. Let the velocity at $r = R$ be

$$v_r)_R = \sum_{n=0}^{\infty} (V_{rn} \cos n\theta + V_{rn}^{*} \sin n\theta) \tag{2.11}$$

and

$$v_\theta)_R = \sum_{n=0}^{\infty} (V_{\theta n} \cos n\theta + V_{\theta n}^{*} \sin n\theta) \tag{2.12}$$

and the velocity at $r \to \infty$ be

$$u)_{r\to\infty} = U_0 - \frac{\zeta}{2}(Y + r \sin\theta) - \dot{X} \tag{2.13}$$

and

$$v)_{r\to\infty} = V_0 + \frac{\zeta}{2}(X + r \cos\theta) - \dot{Y}\ . \tag{2.14}$$

The coefficients V_{rn}, V_{rn}^{*}, $V_{\theta n}$, and $V_{\theta n}^{*}$ are functions of time only and are measured in the moving coordinates, as are $v_r)_R$, $v_\theta)_R$, $u)_\infty$ and $v)_\infty$. U_0 and V_0 are the components of a uniform stream measured at the origin of the fixed coordinate system. The velocity components U and V are the basic current at the center of the hurricane measured in the fixed coordinates and are

$$U = U_0 - \frac{\zeta}{2} Y \tag{2.15}$$

and

$$V = V_0 + \frac{\zeta}{2} X \tag{2.16}$$

and U and V correspond to the steering current for the hurricane. The asymmetry of the lowest order of the wind is caused by the basic current and doublet flow and is contained in the first harmonic, with respect to θ, of the velocity field on $r = R$. Thus let

$$V_{rm} = V_{rm}^* = V_{\theta m} = V_{\theta m}^* = 0 \text{ for } m \geq 2 \,. \tag{2.17}$$

Substitution of (2.11) to (2.17) into (2.7) to (2.10) yields the following relations:

$$\Psi_1 = V_0 - \dot{Y} \,, \tag{2.18}$$

$$\Psi_1^* = - (U_0 - \dot{X}) \,, \tag{2.19}$$

$$\frac{\Psi_{-1}}{R^2} = - (V - \dot{Y}) + V_{r1}^* \,, \tag{2.20}$$

and

$$\frac{\Psi_{-1}^*}{R^2} = U - \dot{X} - V_{r1} \,. \tag{2.21}$$

The last pair of equations may be expressed in terms of v_θ by

$$\frac{\Psi_{-1}}{R^2} = V - \dot{Y} - V_{\theta 1} \tag{2.22}$$

and

$$\frac{\Psi_{-1}^*}{R^2} = - (U - \dot{X}) - V_{\theta 1}^* \,. \tag{2.23}$$

Because (2.20) and (2.21) are identical to (2.22) and (2.23), the following relations occur:

$$V_{r1} = 2(U - \dot{X}) + V^{*}_{\theta 1} \tag{2.24}$$

and

$$V^{*}_{r1} = 2(V - \dot{Y}) - V_{\theta 1} \; . \tag{2.25}$$

Furthermore, (2.17) requires that

$$\Psi_m = \Psi^{*}_m = \Psi_{-m} = \Psi^{*}_{-m} = 0 \text{ for } m \geq 2. \tag{2.26}$$

The results of evaluating the streamfunction coefficients may be collected to give

$$\begin{aligned} v_r = \frac{m}{2\pi r} &+ [(U - \dot{X}) - ((U - \dot{X}) - V_{r1})\frac{R^2}{r^2}] \cos\theta \\ &+ [(V - \dot{Y}) - ((V - \dot{Y}) - V^{*}_{r1})\frac{R^2}{r^2}] \sin\theta \end{aligned} \tag{2.27}$$

and

$$\begin{aligned} v_\theta = \frac{\Gamma + \pi r^2 \zeta}{2\pi r} &+ [(V - \dot{Y}) - ((V - \dot{Y}) - V_{\theta 1})\frac{R^2}{r^2}] \cos\theta \\ &+ [-(U - \dot{X}) + ((U - \dot{X}) + V^{*}_{\theta 1})\frac{R^2}{r^2}] \sin\theta \; . \end{aligned} \tag{2.28}$$

It is convenient to define D and D^{*}, the components of the doublet flow, by

$$D = V_{r1} - (U - \dot{X}) = V_{\theta 1}^{*} + (U - \dot{X}) \tag{2.29}$$

and

$$D^{*} = V_{r1}^{*} - (V - \dot{Y}) = (V - \dot{Y}) - V_{\theta 1} . \tag{2.30}$$

These equations are consistent with (2.24) and (2.25). By using (2.29) and (2.30), the radial and tangential velocity components become

$$v_r = \frac{m}{2\pi r} + [(U - \dot{X}) + D \frac{R^2}{r^2}] \cos\theta + [(V - \dot{Y}) + D^{*} \frac{R^2}{r^2}] \sin\theta \tag{2.31}$$

and

$$v_\theta = \frac{\Gamma + \pi r^2 \zeta}{2\pi r} + [(V - \dot{Y}) - D^{*} \frac{R^2}{r^2}] \cos\theta + [-(U - \dot{X}) + D \frac{R^2}{r^2}] \sin\theta \tag{2.32}$$

so that the symmetric velocity outside R results from the vorticity of the basic current plus the velocity induced by the singular source and vortex at the origin. The non-symmetric velocity is the superposition of a uniform stream and doublet flow. The circulation and source strength are defined by the velocity components by

$$\Gamma = \int_0^{2\pi} v_\theta \, r \, d\theta \tag{2.33}$$

and

$$m = \int_0^{2\pi} v_r \, r \, d\theta . \tag{2.34}$$

These relations define Γ and m in an arbitrary flow field as well as the one given above.

The Geopotential

The geopotential may be represented by

$$\varphi = \sum_{n=0}^{\infty} (\varphi_n \cos n\,\theta + \varphi_n^* \sin n\,\theta) \tag{2.35}$$

where φ_n and φ_n^* are functions of r and t. The coefficients φ_n and φ_n^* are determined from (2.4) and/or by substitution of φ and ψ into (2.1) and matching coefficients.

Certain coefficients appearing on the left hand side of (2.1) do not match geopotential terms on the right. These terms must collectively vanish. This yields two vorticity equations which are

$$\dot{\Gamma} = - m\,(f + \zeta) - \mu\,\Gamma \tag{2.36}$$

and

$$\dot{\zeta} = - \mu\,\zeta \tag{2.37}$$

Generation of positive circulation, $\Gamma > 0$, occurs in (2.36) when a sink, $m < 0$, converts vorticity of the earth and basic current into hurricane circulation. A source, $m > 0$, would destroy positive or cyclonic circulation. There is no generation term analogous to m in (2.37) because there are no divergent winds in the basic current. The influence of surface friction μ is to reduce the circulation and vorticity of (2.36) and (2.37), respectively.

The geopotential coefficients are given by

$$\varphi_0 = \Phi_0 + \frac{(2f+\zeta)}{8}\zeta r^2 - \frac{\Gamma^2+m^2}{8\pi^2 r^2} + \frac{(f+\zeta)\Gamma - \dot{m} - \mu m}{2\pi}\ln r\,, \tag{2.38}$$

$$\begin{aligned}\varphi_1 = {} & [-\ddot{X} + \dot{\Psi}_1^* + (f + \frac{\zeta}{2} - \frac{\Gamma}{2\pi r^2})\Psi_1 + \frac{\zeta}{2}\dot{Y} + \frac{\zeta}{2}(f + \frac{\zeta}{2} - \frac{\Gamma}{2\pi r^2})X \\ & + f\dot{Y} + \frac{\dot{\zeta} Y}{2} - \mu\dot{X} + \mu\frac{\zeta}{2}Y + \mu\Psi_1^*]\,r + [-\dot{\Psi}_{-1}^* \\ & + (f + \frac{3}{2}\zeta + \frac{\Gamma}{2\pi r^2})\Psi_{-1} + \frac{m}{2\pi}(\frac{\zeta}{2}Y + \Psi_1^*) + \frac{m}{2\pi r^2}\Psi_{-1}^* - \mu\Psi_{-1}^*]\frac{1}{r}\,,\end{aligned} \tag{2.39}$$

$$\begin{aligned}\varphi_1^* = {} & [-\ddot{Y} - \dot{\Psi}_1 + (f + \frac{\zeta}{2} - \frac{\Gamma}{2\pi r^2})\Psi_1^* - \frac{\zeta}{2}\dot{X} + \frac{\zeta}{2}(f + \frac{\zeta}{2} - \frac{\Gamma}{2\pi r^2})Y \\ & - f\dot{X} - \frac{\dot{\zeta} X}{2} - \mu\dot{Y} - \mu\frac{\zeta}{2}X - \mu\Psi_1]\,r + [\dot{\Psi}_{-1} \\ & + (f + \frac{3}{2}\zeta + \frac{\Gamma}{2\pi r^2})\Psi_{-1}^* - \frac{m}{2\pi}(\frac{\zeta}{2}X + \Psi_1) - \frac{m\Psi_{-1}}{2\pi r^2} + \mu\Psi_{-1}]\frac{1}{r}\,,\end{aligned} \tag{2.40}$$

$$\varphi_2 = \frac{1}{r^2}[\Psi_{-1}(\frac{\zeta}{2}X + \Psi_1) - \Psi_{-1}^*(\frac{\zeta}{2}Y + \Psi_1^*)]\,, \tag{2.41}$$

$$\varphi_2^* = \frac{1}{r^2}[\Psi_{-1}(\frac{\zeta}{2}Y + \Psi_1^*) + \Psi_{-1}^*(\frac{\zeta}{2}X + \Psi_1)]\,, \tag{2.42}$$

and

$$\varphi_m = \varphi_m^* = 0 \text{ for } m \geq 3. \tag{2.43}$$

By making use of (2.15) through (2.23) and (2.37), the φ_n's may be written in terms of v_r as

$$\varphi_1 = [-\dot{U}_0 + (f + \frac{\zeta}{2}) V - \mu U_0] r - [(f + \frac{3}{2}\zeta + \frac{\Gamma}{2\pi R^2}) \delta V + \delta\dot{U}$$

$$- \dot{V}_{r1} - (f + \frac{3}{2}\zeta) V_{r1}^* + \frac{m}{2\pi R^2} \delta U + \mu (\delta U - V_{r1})] \frac{R^2}{r} \tag{2.44}$$

$$+ [\frac{m}{2\pi R^2} (\delta U - V_{r1}) - \frac{\Gamma}{2\pi R^2} (\delta V - V_{r1}^*)] \frac{R^4}{r^3} ,$$

$$\varphi_1^* = [-\dot{V}_0 - (f + \frac{\zeta}{2}) U - \mu V_0] r - [-(f + \frac{3}{2}\zeta + \frac{\Gamma}{2\pi R^2}) \delta U + \delta\dot{V}$$

$$- \dot{V}_{r1}^* + (f + \frac{3}{2}\zeta) V_{r1} + \frac{m}{2\pi R^2} \delta V + \mu (\delta V - V_{r1}^*)] \frac{R^2}{r} \tag{2.45}$$

$$+ [\frac{m}{2\pi R^2} (\delta V - V_{r1}^*) + \frac{\Gamma}{2\pi R^2} (\delta U - V_{r1})] \frac{R^4}{r^3} ,$$

$$\varphi_2 = [-(\delta V - V_{r1}^*) \delta V + (\delta U - V_{r1}) \delta U] \frac{R^2}{r^2} , \tag{2.46}$$

and

$$\varphi_2^* = [(\delta V - V_{r1}^*)\,\delta U + (\delta U - V_{r1})\,\delta V]\,\frac{R^2}{r^2}\,, \qquad (2.47)$$

where δU and δV are defined by

$$\delta U = U - \dot{X} \quad , \quad \delta V = V - \dot{Y} \qquad (2.48)$$

and $\delta\dot{U}$ and $\delta\dot{V}$ are

$$\delta\dot{U} = \dot{U} - \ddot{X} \quad , \quad \delta\dot{V} = \dot{V} - \ddot{Y}\,. \qquad (2.49)$$

The geopotential in terms of v_θ are

$$\varphi_1 = [-\dot{U}_0 + (f + \frac{\zeta}{2})\,V - \mu\,U_0]r + [(f + \frac{3}{2}\zeta - \frac{\Gamma}{2\pi R^2})\,\delta V + \delta\dot{U}$$

$$+ \dot{V}_{\theta 1}^* - (f + \frac{3}{2}\zeta)\,V_{\theta 1} - \frac{m}{2\pi R^2}\,\delta U + \mu\,(\delta U + V_{\theta 1}^*)]\,\frac{R^2}{r}$$

$$- [\frac{m}{2\pi R^2}\,(\delta U + V_{\theta 1}^*) - \frac{\Gamma}{2\pi R^2}\,(\delta V - V_{\theta 1})]\,\frac{R^4}{r^3}\,, \qquad (2.50)$$

$$\varphi_1^* = [-\dot{V}_0 - (f + \frac{\zeta}{2})\,U - \mu V_0]\,r + [-(f + \frac{3}{2}\zeta - \frac{\Gamma}{2\pi R^2})\,\delta U + \delta\dot{V}$$

$$- \dot{V}_{\theta 1} - (f + \frac{3}{2}\zeta)\,V_{\theta 1}^* - \frac{m}{2\pi R^2}\,\delta V + \mu(\delta V - V_{\theta 1})]\,\frac{R^2}{r}$$

$$- \left[\frac{m}{2\pi R^2} (\delta V - V_{\theta 1}) + \frac{\Gamma}{2\pi R^2} (\delta U + V_{\theta 1}^*) \right] \frac{R^4}{r^3} \quad , \tag{2.51}$$

$$\varphi_2 = [- (\delta U + V_{\theta 1}^*) \, \delta U + (\delta V - V_{\theta 1}) \, \delta V] \frac{R^2}{r^2} \quad , \tag{2.52}$$

and

$$\varphi_2^* = [- (\delta V - V_{\theta 1}) \, \delta U - (\delta U + V_{\theta 1}^*) \, \delta V] \frac{R^2}{r^2} \; . \tag{2.53}$$

It is useful to introduce D and D^* into φ_1 and φ_1^* because (2.44) and (2.50) and (2.45) and (2.51) have a single form given by

$$\varphi_1 = [- \dot{U}_0 + (f + \frac{\zeta}{2}) V - \mu U_0] \, r + [- \frac{\Gamma}{2\pi R^2} \delta V + (f + \frac{3}{2}\zeta) \, D^*$$

$$+ \dot{D} - \frac{m}{2\pi R^2} \delta U + \mu D] \frac{R^2}{r} + [\frac{\Gamma}{2\pi R^2} D^* - \frac{m}{2\pi R^2} D] \frac{R^4}{r^3} \tag{2.54}$$

and

$$\varphi_1^* = [- \dot{V}_0 - (f + \frac{\zeta}{2}) U - \mu V_0] \, r + [\frac{\Gamma}{2\pi R^2} \delta U - (f + \frac{3}{2}\zeta) \, D$$

$$+ \dot{D}^* - \frac{m}{2\pi R^2} \delta V + \mu D^*] \frac{R^2}{r} - [\frac{\Gamma}{2\pi R^2} D + \frac{m}{2\pi R^2} D^*] \frac{R^4}{r^3} \tag{2.55}$$

In the discussions to follow, φ_1 and φ_1^* are given prime importance because only these components may give a net force upon the hurricane circulation. The most fundamental expressions for φ_1 and φ_1^* may be (2.54) and (2.55) where the geopotential is given in terms of parameters describing the elementary flow fields representing the symmetric and non-symmetric parts of the hurricane vortex and the basic current. Physical interpretation of the individual terms is most clear and these equations clearly show that the hurricane acceleration does not appear in the geopotential. $\ddot{X}$ and $\ddot{Y}$ appear only if $\dot{V}_{r1}$ and $\dot{V}_{r1}^*$ or $\dot{V}_{\theta 1}$ and $\dot{V}_{\theta 1}^*$ are zero, the former being the condition appropriate for a solid cylinder of radius R.

The geopotential distribution of this model is the union of circular contours of φ_0, parallel and doublet or dipole configurations of φ_1 and φ_1^*, and the quadrapole structure of φ_2 and φ_2^*. Considering φ_1 and φ_1^*, the first group of terms proportional to r give parallel straight contours, the second is a simple dipole and the last is a dipole proportional to r^{-3}.

The first term of the straight contour group gives the balance between the geopotential and the acceleration of the basic current $\dot{U}_0$. Note that $\dot{U}$ does not appear here and this is because U differs from U_0 by the addition of a pure rotational flow whose changes are governed by (2.37). A similar remark applies to the friction terms. Actually, by use of (2.37), the steering current U can be introduced, but an extra term results whose interpretation is obscure. The middle terms, $(f + \frac{\zeta}{2})V$ and $-(f + \frac{\zeta}{2})U$, combine with the second term of φ_0 to give circular contours balancing the solid rotation centered at the origin in the fixed coordinates ($X = Y = 0$), plus straight contours giving the Coriolis balance for U_0 and V_0.

The first term of the simple dipole group represents the magnus effect which gives the rotor or Kutta-Joukowski force on a solid cylinder. The second term is the interaction of the doublet flow and rotation due to the earth and fluid vorticity. The third term gives the balance with the doublet acceleration which, in contrast to $\dot{\Gamma}$, is induced directly by the geopotential. The fourth term is the interaction between the source m and the relative basic current. The last term balances the surface friction for the doublet flow. The last group of geopotential terms proportional to r^{-3} give the magnus effect for the doublet flow and the interaction of the source and doublet.

At this point, it is convenient to note the relative size or importance of the terms appearing in (2.54) and (2.55) and to anticipate some results of the data to be discussed below. With respect to the rotational motion, there appear parameters f, ζ and Z where $Z = \Gamma/2\pi R^2$. These quantities have the dimension of reciprocal of time, or T^{-1}. By using the concept of scale analysis, these quantities may be estimated, except f which has intrinsic values for each latitude circle. By choosing a velocity LT^{-1} and a length L typical of the type of motion of interest, the time scale T or its reciprocal may be estimated.

For the large-scale or environment flow in the tropics, choose a velocity of 10 m sec^{-1} and length of 1000 km. This gives a scale for $\zeta \approx 10^{-5}$ sec^{-1}. For the hurricane circulation, a velocity of 50 m sec^{-1} and length of 100 km correspond to a typical maximum wind and diameter of the maximum wind belt giving an estimate of $Z \approx 5 \times 10^{-4}$ sec^{-1}. Data for tropical storm Betsy give a range of Z of 2 to 5×10^{-4} sec^{-1}. The Coriolis parameter f is $5 \times 10^{-5} sec^{-1}$ at 20^{o}N latitude.

Thus, Z is about one order of magnitude larger than f, which is an order larger than ζ. Since U_0, V_0, D, D^*, $\dot{X}$ and $\dot{Y}$ are near the same size, it is apparent that Z terms are largest, f next, and ζ last. Since ζ appears in combination with f and is less than one-fifth of f, it is reasonable to neglect ζ. In doing so, the distinction between U and U_0 vanishes.

The quantity $m/2\pi R^2$ has the dimension of T^{-1} and represents the symmetric flow of air in or out of the hurricane which takes place inward near the ground (0 to 2000 m) and outward in the upper troposphere (10,000 to 15,000 m). For an inflow of 10 m sec^{-1} at 100 km, $m/2\pi R^2 \approx 10^{-4} sec^{-1}$ so that this term may be important in the boundary layer or outflow. The data for Betsy are at 11,780 feet ($\sim$3300 m) where the symmetric inflow is about 1 m sec^{-1} at 100 km so that $m/2\pi R^2$ has the scale of ζ and will be neglected. Values for μ to apply to data for 11,780 feet are not very well known, and these terms will not be estimated. It is expected that this will not cause any difficulty in interpreting the results of computations to follow.

The forementioned simplifications lead to equations for the geopotential in terms of v_r

$$\varphi_1 = (- \dot{U}_0 + fV_0)\ r + [- Z\delta V + f\ (V_{r1}^* - \delta V) + \dot{V}_{r1} - \delta\dot{U}]\ \frac{R^2}{r}$$

$$+ Z\ (V_{r1}^* - \delta V)\ \frac{R^4}{r^3}\ , \qquad (2.56)$$

and

$$\varphi_1^* = (-\dot{V}_0 - fU_0)\ r + [Z\delta U + f(\delta U - V_{r1}) + \dot{V}_{r1}^* - \delta\dot{V}]\ \frac{R^2}{r}$$

$$- Z\ (V_{r1} - \delta U)\ \frac{R^4}{r^3}\ , \qquad (2.57)$$

and in terms of v_θ

$$\varphi_1 = (-\dot{U}_0 + fV_0)\ r + [-Z\delta V + f(\delta V - V_{\theta 1}) + \dot{V}_{\theta 1}^* + \delta\dot{U}]\ \frac{R^2}{r}$$

$$+ Z\ (\delta V - V_{\theta 1})\ \frac{R^4}{r^3}\ , \qquad (2.58)$$

and

$$\varphi_1^* = (-\dot{V}_0 - fU_0)\ r + [Z\delta U - f(\delta U + \dot{V}_{\theta 1}^*) - \dot{V}_{\theta 1} + \delta\dot{V}]\ \frac{R^2}{r}$$

$$- Z\ (\delta U - V_{\theta 1}^*)\ \frac{R^4}{r^3}\ , \qquad (2.59)$$

and in terms of D and D^*

$$\varphi_1 = (-\dot{U}_0 + fV_0)\ r + (-Z\delta V + fD^* + \dot{D})\ \frac{R^2}{r} + ZD^*\ \frac{R^4}{r^3}\ , \qquad (2.60)$$

and

$$\varphi_1^* = (-\dot{V}_0 - fU_0)\ r + (Z\delta U - f\dot{D} + \dot{D}^*)\ \frac{R^2}{r} - ZD\ \frac{R^4}{r^3}\ . \qquad (2.61)$$

These equations form the basis of the discussion of the balance of wind and geopotential in Chapters III and IV.

It is thought that the model given here is the most general possible in which solutions of (2.1) are given by the simple analytic functions used here. Attempts to include spare variation of f, ζ or μ do not lead to solutions of the type given here.

CHAPTER III

ANALYSIS OF DATA

Analysis of Wind and Geopotential

This chapter discusses the analysis of the research flight data for Tropical Storm Betsy collected by the National Hurricane Research Laboratory. In the second section of the chapter, the computation of the basic current from the aircraft wind data is discussed. This computation involves the question of fitting the observed wind data to the model wind fields of Chapter II.

At the time of observation, Betsy was located near 20°N latitude and 65°W longitude, as may be seen in Fig. 1 where the tropical storm tracks of 1965 are shown for the Atlantic Ocean and adjacent areas. The aircraft flight path, plotted with respect to the moving storm center, is shown in Fig. 3 with the time along the path given in 10 minute intervals. Data were recorded every five seconds along this path, but only two-minute intervals were plotted and used to construct the wind and geopotential analyses. As may be seen, data appear in all quadrants of the storm, both along radial legs and on a circumnavigation path. Near the center, data are plentiful but also vary considerably with time so that analysis of a mean field is questionable. Beyond 50 km, time variations appear but are much smaller than variations near the center, and a meaningful time average analysis is possible.

An important problem may influence the analysis of time composited data when the strength of a storm is changing significantly. If the central pressure or geopotential is rising or falling rapidly, a false asymmetry is recorded by an aircraft flying diametrically across the storm. Fig. 2 shows the trace of central pressure for Betsy and it is noted that the pressure is falling rapidly between 1200 and 1800 GMT. Data collected between 1600 and 1800 GMT show higher geopotential values where subsequent data overlap these data, but overlapping data collected after 1830 agree with each other. Use of the 1600-1800 GMT data would change the asymmetry of the geopotential. The latter data are accepted here because they are recorded during a time of slowly varying central pressure. This condition is required for a meaningful time average geopotential analysis. The wind observations were examined also and, as discussed in Chapter V, significant changes are observed. But, results of computations there suggest that the non-symmetric wind is changing slowly in time, and it is the symmetric wind which accounts for most of the change in response to the lower central pressure noted above. The critical question is whether the basic current is seriously affected by time change of the wind. The belief is that it is not because the patterns of inflow and outflow and wind speed which govern the basic current appear similar at all times so that a meaningful time average can be constructed.

Data giving the observed velocity of Betsy between 1530 and 2330 GMT on 29 August 1965 appear in Table 1. Data are reported to the nearest degree and knot for the time intervals indicated. The eastward and northward velocity components, $\dot{X}$ and $\dot{Y}$, in meters per second, are given from the velocity reported at each time interval. Some irregularity of $\dot{X}$ and $\dot{Y}$ may be noted because of the steps of speed and direction.

Minor oscillations of the track of a hurricane are often observed and, because no important change of direction of Betsy's path is evident in Fig. 1 at this time, it may be reasonable to treat the motion recorded in Table 1 as the superposition of a mean motion and an oscillation. The mean motion is taken to be toward 330 degrees, partly for convenience and because the geopotential data which will be used to discuss the acceleration of Betsy were observed between 1830 and 2330 GMT. In any event, the mean motion is close to 330 degrees. The mean acceleration of Betsy may be computed for the duration of each of the speeds from 11 to 7 knots by assuming that a one knot decrease occurs for these time periods in the direction of 150 degrees. The x and y components of the mean acceleration, $\overline{\ddot{X}}$ and $\overline{\ddot{Y}}$, are given in Table 2 for the time intervals indicated and for the time intervals 1801 to 2110 and 1601 to 2110 GMT.

From the data of Tables 1 and 2, it is evident that Betsy is decelerating through most of the observation period, except perhaps at the end. The deceleration rate diminishes by more than a factor of two. This creates difficulties in relating the acceleration of Betsy to the observed wind and geopotential analyses which are time averages. The time average geopotential field, which may give the force accelerating the storm, is based upon data collected between 1830 and 2330 GMT so that the acceleration of the storm reflected in these data may be either the values computed for 1801-2110 or 1903-2110 GMT.

The geopotential φ is determined by using the pressure data observed along the flight path of Fig. 3. The pressure data are corrected from the level at which the aircraft was flying (12,400 to 13,300 feet) to a standard reference level of 11,780 feet by the National Hurricane Research Laboratory and reported as "D" values. The "D" value is the difference between the height of the pressure observation (11,780) and the height in the standard atmosphere at which the same pressure occurs. The units of "D" are given in geopotential meters, and this is converted to φ of our model by multiplication by the acceleration of gravity, 9.8 m sec^{-2}. It should be noted that the geopotential, defined in this paper for a homogeneous fluid, is equivalent to pressure but differs from the customary use of the term in meteorology where vertical distances are measured in units of geopotential, referring to the potential energy per unit mass resulting from the earth's gravity. In meteorological use, the geopotential at 11,780 feet is uniform. The units are the same, $m^2 sec^{-2}$. It should also be noted that the pressure force in (2.1) is an approximation to the horizontal pressure force per unit mass observed in the atmosphere because density varies in the atmosphere.

The analysis of the geopotential was done to emphasize the zero and first harmonics of the geopotential and to suppress higher harmonics. The variability of the data along the flight path makes reliable analysis of the high harmonics questionable. As pointed out above, only data collected after 1831 GMT were accepted for the geopotential analysis, but data collected before this time were partly accounted for by analyzing them for the gradient of φ along radial legs. The geopotential analysis within 50 km represents an approximate time average of changing conditions and may not be very reliable. The geopotential analysis appears in Fig. 4. The most important result of the analysis is the asymmetric geopotential showing high values in the northwest quadrant and low values in the southeast quadrant of the storm.

The winds observed, with respect to the earth's surface, along the path in Fig. 3 were analyzed by resolving them into isogons and isotachs. The higher harmonics of the wind were suppressed in the analysis. Where overlapping data occur, the average wind was analyzed. The variability of the wind inside 50 km makes the analysis here very approximate and, to some extent, it represents an inward extrapolation of patterns. The isogon and isotach fields are shown in Figs. 5 and 6, respectively, and, superposed on the isogon field is a streamline analysis constructed from the isogon analysis. The isogon analysis was given precedence over the streamlines because it is far easier to control the spacing of isogons, which determines the change of curvature of the streamlines, than it is to directly control the curvature changes of the streamlines as they are determined from the observed wind field. Thus, filtering of higher harmonics of the wind is easier to accomplish in the isogon field. The streamline analysis best shows the pattern of inflow of air in the north and west quadrants and the outflow in the east quadrant. This inflow-outflow pattern is very important because it results in a basic current directed toward the southeast. The streamlines indicate that a net inflow of air may be occurring. Computation of the symmetric radial wind gives net inflow of 1.48, 1.14, 0.77 and 0.30 m sec^{-1} at 125, 100, 75 and 50 km, respectively.

To compute the harmonic components of the wind and geopotential, which were introduced in Chapter II, data were tabulated at radial intervals of 12.5 km at each 15 degrees about a circle out to a radius of 125 km. These data were resolved into harmonic components at each radius by use of a computer program written by Dr. John M. Lewis. Since the wind data of Figs. 5 and 6 are measured with respect to a coordinate system fixed in the earth's surface, while the harmonic wind components V_{r1}, V^*_{r1}, $V_{\theta 1}$, and $V^*_{\theta 1}$, are measured in a coordinate system moving with the storm center, it is necessary to add the storm velocity to the observed winds. Mean storm velocities of 330° 9 kt and 330° 6 kt were used. The harmonic coefficients for the first harmonic appear in Table 3, the second harmonic in Table 4, and the storm velocity is 330° 9 kt. The storm velocity components are $\bar{\dot{X}} = -2.32$ m sec^{-1} and $\bar{\dot{Y}} = 4.01$ m sec^{-1} and, if these values are added to V_{r1} and V^*_{r1}, respectively, it is noted that inflow is shown in the northwest and outflow in the southeast quadrants of the storm.

Computation of the Basic Current

The basic current is expressed in terms of the first harmonic wind coefficients through (2.24) and (2.25). It is given by

$$U_0 = \dot{X} + \tfrac{1}{2}(V_{r1} - V^*_{\theta 1}) \tag{3.1}$$

and

$$V_0 = \dot{Y} + \tfrac{1}{2}(V^*_{r1} + V_{\theta 1}) \tag{3.2}$$

where it has been assumed that $\zeta = 0$. Substitution of the data of Table 3 into (3.1) and (3.2), taking care to use values of $\dot{X}$ and $\dot{Y}$ appropriate for a mean storm velocity of 330° 9 kt, gives the basic current values in the left two columns of Table 5. The results are the average x and y components of the observed winds integrated about the corresponding circle. This may be verified by integration of (2.7) and (2.8) with $\zeta = 0$.

If the observed wind fields corresponded exactly to the model wind fields, the same pair of values of U_0 and V_0 would occur at each radius and they would equal the environment steering current. The results in Table 5 fulfill neither of these conditions, so the observed wind fields do not correspond to the model. One way of looking at this is to notice that the model winds, excepting the symmetric wind induced by ζ, are non-divergent and irrotational everywhere except at the origin of the moving coordinate. The divergence and curl of a vector $\underline{V}$ in polar coordinates are

$$\nabla \cdot \underline{V} = \frac{1}{r}\frac{\partial}{\partial r} r v_r + \frac{1}{r}\frac{\partial}{\partial \theta} v_\theta \tag{3.3}$$

and

$$\nabla \times \underline{V} = \frac{1}{r}\frac{\partial}{\partial r} r v_\theta - \frac{1}{r}\frac{\partial}{\partial \theta} v_r . \tag{3.4}$$

The result can be verified by substitution from (2.31) and (2.32). The same exercise performed upon the observed wind fields (discussion below leads to analytic representations for v_r and v_θ) shows that they do not satisfy this condition.

The basic current implied by the model wind field of (2.31) and (2.32) is computed from (3.1) and (3.2) by using the first harmonic wind coefficients, representing the non-divergent and irrotational observed wind. These coefficients may be obtained by computing the divergent and rotational parts of the observed coefficients and by removing these parts. A computation for this is given below. The advantage of computing the basic current in this way is that the non-divergent irrotational basic current is uniform over the disk for which it is computed, whereas the basic current using the observed coefficients is defined only on the boundary of the corresponding circle, but not over the interior. This means that the non-divergent irrotational basic current is determined by divergence and vorticity distributions outside the disk over which it is computed; whereas, the basic current from the observed coefficients is partly controlled by divergence and vorticity inside the circle over which it is computed. This does not mean, as results will show below, that the non-divergent irrotational basic current will agree with the environment steering current. Vorticity and divergence distributions between 125 km and the outside of the storm may cause a disagreement between the basic current and the steering current.

One difficulty is introduced by use of the non-divergent irrotational basic current. According to (2.29) and (2.30), there are two definitions for D and D^*, but these definitions give identical results only if the observed winds correspond exactly to the model, which they do not, or if (3.1) and (3.2), together with the observed harmonic coefficients, define U_0 and V_0. The latter assertion follows from (2.29) and (2.30) which show that the model winds satisfy

$$D = \tfrac{1}{2}(V_{r1} + V_{\theta 1}^{*}) \tag{3.5}$$

and

$$D^{*} = \tfrac{1}{2}(V_{r1}^{*} - V_{\theta 1}) \tag{3.6}$$

and if (3.1) and (3.2) are introduced into either definition of D or D^*, (3.5) or (3.6) follows. Use of non-divergent irrotational coefficients in (3.1) and (3.2) to compute U_0 and V_0 leads to two different values for each of D and D^* if the observed values of V_{r1}, V_{r1}^*, $V_{\theta 1}$ and $V_{\theta 1}^*$ are used in (2.29) and (2.30). If non-divergent irrotational values of the last four coefficients computed on a disk are used, the result is zero for D and D^*, but this is because the doublet flow is singular at the origin so it cannot exist on a disk. Properly, the doublet flow components should be computed from data extending far outside of the disk, but this is not possible in the present case. Or, it is possible to obtain non-divergent irrotational doublet flow coefficients by excluding the origin from the computations.

At this point, it is clear that a compromise must be introduced if the aircraft data are to be fitted to the wind model of Chapter II. Since the object is to compute φ_1 and φ_1^*, it is desirable to have one definition of D and D^*, one computed set of φ_1 and φ_1^*, and to include as much of the observed wind in the computations as possible. The compromise introduced here is to compute U_0 and V_0 from (3.1) and (3.2) with non-divergent and irrotational wind coefficients computed on a disk and to compute D and D^* from (3.5) and (3.6) with the observed wind coefficients. Then φ_1 and φ_1^* are computed from (2.60) and (2.61), but notice that the average φ_1 and φ_1^* computed from (2.56) to (2.59), where the differing D and D^* expressions are used, are just (2.60) and (2.61), provided D and D^* are given respectively by (3.5) and (3.6). This compromise retains the uniform property of U_0 and V_0 over the disk, and this is important in subsequent discussion of the basic current in Chapters V and VI.

The basic current is non-divergent and irrotational and is computed by removing the divergent and rotational parts of the wind field from the observed winds. This may be done following a variational method discussed by Sasaki (1958). The approach is to minimize the variance between the observed wind field, V_r^0 and V_θ^0, and the non-divergent irrotational winds, V_r and V_θ, subject to the constraint that the divergence and curl of V_r, V_θ, vanish. This is accomplished by minimizing the function,

$$\int_A [(V_r - V_r^0)^2 + (V_\theta - V_\theta^0)^2 + 2\varphi\nabla \cdot \underline{V} + 2\lambda\nabla \times \underline{V}]\, dA \qquad (3.7)$$

where the components of $\underline{V}$ are V_r and V_θ, the integration extends over a circle and φ and λ are Lagrange multipliers.

The results of minimizing (3.7) with respect to the unknown functions are

$$\delta(V_r) : \qquad V_r = V_r^0 + \frac{\partial\varphi}{\partial r} - \frac{1}{r}\frac{\partial\lambda}{\partial\theta}, \qquad (3.8)$$

$$\delta(V_\theta) : \qquad V_\theta = V_\theta^0 + \frac{1}{r}\frac{\partial\varphi}{\partial\theta} + \frac{\partial\lambda}{\partial r}, \qquad (3.9)$$

$$\delta(\varphi) : \qquad \nabla \cdot \underline{V} = 0 , \tag{3.10}$$

and

$$\delta(\lambda) : \qquad \nabla \times \underline{V} = 0 . \tag{3.11}$$

The equations for φ and λ are obtained by substituting (3.8) and (3.9) into (3.10) and (3.11), giving

$$\nabla^2\varphi = - \nabla \cdot \underline{V}^0 \tag{3.12}$$

and

$$\nabla^2\lambda = - \nabla \times \underline{V}^0 . \tag{3.13}$$

Thus, φ and λ are the negative, respectively, of the velocity potential for irrotational flow and the streamfunction for non-divergent flow. The boundary conditions to insure the minimum of (3.7) in polar coordinates are

$$\varphi \; \delta(V_r) = 0 \quad \text{at } r = R \tag{3.14}$$

and

$$\lambda \; \delta(V_\theta) = 0 \quad \text{at } r = R . \tag{3.15}$$

These conditions are satisfied by choosing $\varphi = \lambda = 0$ on the boundary. The basic current, U_0 and V_0, is obtained by solving (3.12) and (3.13) for the first harmonic of the wind field and by evaluating (3.8) and (3.9) for the same harmonic. This yields a uniform stream over a circle. If higher harmonics of the wind are involved, the solution for each harmonic is a corner flow with the angle given by πn^{-1}, where n is the wave number.

The basic current may be calculated either by following the analytical or numerical method. The analytic approach is represented below. The relative, radial and tangential wind harmonic coefficients may be used to construct an analytic function to represent the observed wind on a circle in which the radial variation of the wind is given by a polynomial in r and the angular variation is expressed by trigonometric functions. Let

$$V_r^{\,0} = \sum_{n=0}^{N} \left\{ \left(\sum_{m=0}^{M} a_{mn} r^m \right) \cos n\theta + \left(\sum_{m=0}^{M} a_{mn}^{*} r^m \right) \sin n\theta \right\} \qquad (3.16)$$

and

$$V_\theta^{\,0} = \sum_{n=0}^{N} \left\{ \left(\sum_{m=0}^{M} b_{mn} r^m \right) \cos n\theta + \left(\sum_{m=0}^{M} b_{mn}^{*} r^m \right) \sin n\theta \right\} \qquad (3.17)$$

The divergence and vorticity are

$$\nabla \cdot \underline{V}^0 = \sum_{n=0}^{N} \left\{ \sum_{m=0}^{M} \left[(m+1)\, a_{mn} + n\, b_{mn}^{*} \right] r^{m-1} \cos n\theta \right.$$

$$\left. + \sum_{m=0}^{M} \left[(m+1)\, a_{mn}^{*} - n\, b_{mn} \right] r^{m-1} \sin n\theta \right\}, \qquad (3.18)$$

and

$$\nabla \times \underline{V}^0 = \sum_{n=0}^{N} \{ \sum_{m=0}^{M} [(m+1)\, b_{mn} - n\, a_{mn}^*]\, r^{m-1} \cos n\theta$$

$$+ \sum_{m=0}^{M} [(m+1)\, b_{mn}^* + n\, a_{mn}]\, r^{m-1} \sin n\theta \}. \qquad (3.19)$$

When m = 0, a singularity exists at the origin of both the divergence and vorticity unless conditions are imposed upon the coefficients of (3.16) and (3.17). The singularities are removed by imposing

$$a_{00} = b_{00} = 0 \;,\; n = 0$$

$$\left. \begin{aligned} a_{01} &= - b_{01}^* \\ a_{01}^* &= b_{01} \end{aligned} \right\} \; n = 1 \qquad (3.20)$$

and $a_{0n} = a_{0n}^* = b_{0n} = b_{0n}^* = 0$ for $n > 1$.

The coefficients of (3.16) and (3.17) are computed by fitting a polynomial to the observed harmonic components of the wind field which have been computed for ten radii. For example, let

$$A(r) = \sum_{m=0}^{M} a_{mn} r^m \;, \qquad (3.21)$$

The a_{mn}'s are obtained by minimizing the variance between A(r) and the harmonic wind coefficients at ten radii. Thus,

$$\sum_{i=1}^{10} [A(r_i) - V_{rni}]^2 = \min \tag{3.22}$$

determines the polynomial fitting the cosine harmonic of the relative radial wind. Taking note of (3.20), the remaining a_{mn}'s are determined by

$$\sum_{i=1}^{10} \sum_{m=1}^{M} a_{mn}\, r_i^m\, r_i^p = \sum_{i=1}^{10} (V_{rni} - a_{0n})\, r_i^p \tag{3.23}$$

where p = 1, 2, . . . M and a separate set of (3.23) applies for each n. The coefficients a^*_{mn} are determined by V^*_{rn}, b_{mn} by $V_{\theta n}$, and b^*_{mn} by $V^*_{\theta n}$. The values of M must be between 1 and 10. Even though M = 10 would fit A(r) exactly to the data points, experience shows that such a polynomial deviates far from the expected values of the data between points. To obtain a smooth approximating polynomial, M = 4 was selected.

Fulfillment of (3.20) requires a wind observation at r = 0 or the storm center, the x-component of which is V_{r1} or $-V^*_{\theta 1}$, and the y-component of which is V^*_{r1} or $V_{\theta 1}$. Because of the presence of the eye of the storm, the observed wind at r = 0 is variable in time and averages near zero. The object of fitting the wind data by a polynomial is to obtain a good approximation outside the eye of the storm, and this purpose is best served by choosing a_{01} to be the average value of V_{r1} plus $-V^*_{\theta 1}$, observed at 12.5 km, and having a^*_{01} be given by the average of V^*_{r1} plus $V_{\theta 1}$, observed at 12.5 km. This procedure avoids the large change of $A(r)$ between the origin and 12.5 km which would occur if a_{01} and a^*_{01} were set to zero to simulate the presence of the eye. The results of fitting the first harmonic of the wind field by a quartic polynomial are given in Table 6, where the harmonic coefficients determined by the polynomial appear. Comparing these results to the observed data in Table 3 shows a reasonable fit to the data.

The solutions of (3.12) and (3.13) are most easily obtained by the method of Greens functions. Let $G(r, \theta, r', \theta')$ denote the Greens function. The solutions for φ and λ

$$\varphi(r, \theta) = \int_0^{2\pi} \int_0^R G(r, \theta, r', \theta') \nabla \cdot \underline{V}^0 \, r'dr'd\theta' \tag{3.24}$$

and

$$\lambda(r, \theta) = \int_0^{2\pi} \int_0^R G(r, \theta, r', \theta') \nabla \times \underline{V}^0 \, r'dr'd\theta' \tag{3.25}$$

where G is the solution of

$$\nabla^2 G = -\frac{1}{r} \delta(r - r') \delta(\theta - \theta') \tag{3.26}$$

and the boundary condition $G = 0$ at $r = R$. The right hand side of (3.26) is the Dirac delta function in polar coordinates. The Greens function satisfying these conditions is

$$G(r, \theta, r', \theta') = - \ln \frac{r_>}{R} +$$

$$\sum_{n=1}^{\infty} \frac{1}{2\pi n} \left[\left(\frac{r_<}{r_>} \right)^n - \left(\frac{rr'}{R^2} \right)^n \right] \cos [n(\theta - \theta')] \tag{3.27}$$

where $r_>$ denotes the larger of r or r' and $r_<$ denotes the smaller of r or r'.

The solutions for φ and λ are

$$\varphi = \sum_{m=1}^{M} a_{m0} \frac{R^{m+1}}{m+1} \left[1 - \left(\frac{r}{R} \right)^{m+1} \right] +$$

$$\sum_{n=1}^{N} \left[\sum_{m=1}^{M} \left((m+1)\, a_{mn} + n b^*_{mn} \right) r^n \left(\frac{R^{m-n+1}}{(m-n+1)} - \frac{r^{m-n+1}}{(m+n+1)} \right) \cos n\theta \right. \tag{3.28}$$

$$\left. + \sum_{m=1}^{M} \left((m+1)\, a^*_{mn} - n b_{mn} \right) r^n \left(\frac{R^{m-n+1}}{(m-n+1)} - \frac{r^{m-n+1}}{(m+n+1)} \right) \sin n\theta \right]$$

and

$$\lambda = \sum_{m=1}^{M} b_{m0} \frac{R^{m+1}}{m+1} \left[1 - \left(\frac{r}{R} \right)^{m+1} \right] +$$

$$\sum_{n=1}^{N} \left[\sum_{m=1}^{M} \left((m+1)\, b_{mn} - n a^*_{mn} \right) r^n \left(\frac{R^{m-n+1}}{(m-n+1)} - \frac{r^{m-n+1}}{(m+n+1)} \right) \cos n\theta \right. \tag{3.29}$$

$$\left. + \sum_{m=1}^{M} \left((m+1)\, b^*_{mn} + n\, a_{mn} \right) r^n \left(\frac{R^{m-n+1}}{(m-n+1)} - \frac{r^{m-n+1}}{(m+n+1)} \right) \sin n\theta \right].$$

By substituting (3.16), (3.17), (3.28) and (3.29) into (3.8) and (3.9), and by writing the results for the first harmonic of the wind only, we obtain

$$V_r' = \sum_{m=0}^{M} \frac{(a_{m1} - b_{m1}^*)}{m+2} R^m \cos\theta$$

$$+ \sum_{m=0}^{M} \frac{(a_{m1}^* + b_{m1})}{m+2} R^m \sin\theta , \qquad (3.30)$$

and

$$V_\theta' = \sum_{m=0}^{M} \frac{(a_{m1}^* + b_{m1})}{m+2} R^m \cos\theta$$

$$- \sum_{m=0}^{M} \frac{(a_{m1} - b_{m1}^*)}{m+2} R^m \sin\theta \qquad (3.31)$$

where the prime on V_r and V_θ denote the first harmonic. The basic current is given by

$$U_0 = \dot{X} + \sum_{m=0}^{M} \frac{(a_{m1} - b_{m1}^*)}{m+2} R^m \qquad (3.32)$$

and

$$V_0 = \dot{Y} + \sum_{m=0}^{M} \frac{(a_{m1}^* + b_{m1})}{m+2} R^m . \qquad (3.33)$$

The basic current is uniform inside of R but changes if R is changed. The basic current changes with R because the vorticity and divergence outside of R, which govern U_0 and V_0, is changed by moving R.

The results of computing U_0 and V_0 from (3.32) and (3.33) for various values of R are given in the right hand columns of Table 5. The basic current computed here is opposite to that expected if the hurricane is viewed as a symmetric vortex moving in a steering current. The observed wind is, however, greater on the right than on the left side of the storm, looking in the direction of the motion of the storm, as may be verified in Fig. 6. An interpretation of the basic current computed here is given in Chapter VI where the problem of the motion of the storm is discussed.

CHAPTER IV

BALANCE OF WIND AND GEOPOTENTIAL

The objective of this chapter is to examine the balance of wind and geopotential following the equations developed in Chapter II and utilizing the data of Chapter III. In addition to data tabulated above, values for D, D^* and Z are required. According to (2.33) and the definition of $Z = \Gamma/2\pi R^2$, the values of Z are obtained from

$$Z = \frac{v_{\theta 0}}{R} \quad . \tag{4.1}$$

Values of D and D^* are computed from (3.5) and (3.6). Table 7 contains $v_{\theta 0}$, Z, D, and D^* for each radius.

Corresponding to the choice of U, V, D and D^* above, it is appropriate to compute the balance of wind and geopotential from (2.60) and (2.61). It is convenient to consider this balance at each radius R by utilizing parameters for that radius. For parameters at a particular radius R, (2.60) and (2.61) may be written

$$\frac{\varphi_1}{R} = - \dot{U}_0 + fV_0 + Z(D^* - \delta V) + fD^* + \dot{D} \tag{4.2}$$

and

$$\frac{\varphi_1^*}{R} = - \dot{V}_0 - fU_0 + Z(\delta U - D) - fD + \dot{D}^* . \qquad (4.3)$$

Tropical storm Betsy was near $20^{\circ}N$ so that $f = 5 \times 10^{-5} sec^{-1}$. There are no observed values of the accelerations appearing in (4.2) and (4.3). Numerical values for the remaining terms in (4.2) are given in Table 8 and in (4.3) in Table 9. Since the magnus terms depend upon the velocity of the storm, two values of these terms are given, one for a mean storm velocity of 330° 9 kt, the second at 330° 6 kt.

The most important result shown in Tables 8 and 9 is that the wind and geopotential fields are not in a state of balance. It is not likely that this is the result of either poor data or model simplifications. According to (4.2) and (4.3), the imbalance of wind and geopotential may be interpreted in terms of the acceleration of the model wind fields $\dot{U}_0$, $\dot{V}_0$, $\dot{D}$, and $\dot{D}^*$, but acceleration of the tropical storm is not involved.

The sum $\dot{U}_0 + \dot{D}$ or $\dot{V}_0 + \dot{D}^*$ is all that results from (4.2) and (4.3) unless an assumption is made with respect to the geopotential distribution. Since $\dot{U}_0$ and $\dot{V}_0$ are proportional to the unbalanced uniform geopotential gradient, while $\dot{D}$ and $\dot{D}^*$ arise from a doublet field, it may be reasonable to separate φ_1 and φ_1^* into a uniform gradient plus a residual to be identified with the doublet structure. Two views of the non-symmetric geopotential are shown, one in Fig. 7 where the contours appear, and the other in Fig. 8 where the profiles of φ_1 and φ_1^* appear. These figures suggest that a uniform geopotential gradient exists, directed toward southeast with a superposed disturbance whose amplitude maximum occurs near 290° 50 km. Unfortunately, there is no unique way to determine the uniform gradient but, because Fig. 7 appears to be dominated by it, an approximation to this field is taken to be $\varphi_1/R = -3.05 \times 10^{-4} m^2 sec^{-1}$ and $\varphi_1^*/R = 3.8 \times 10^{-4} m^2 sec^{-1}$. This approximation is taken to give greatest consideration to the data between 100 and 125 km. Lines corresponding to these values appear in Fig. 8. This geopotential governs $\dot{U}_0$ and $\dot{V}_0$ which are calculated from

$$\dot{U}_0 = 3.05 \times 10^{-4} + fV_0 \tag{4.4}$$

and

$$\dot{V}_0 = -3.8 \times 10^{-4} - fU_0 \ . \tag{4.5}$$

The doublet accelerations are given by

$$\dot{D} = \varphi_1/R + 3.05 \times 10^{-4} + Z\delta V - (f + Z)\ D^* \tag{4.6}$$

and

$$\dot{D}^* = \varphi_1^*/R - 3.8 \times 10^{-4} - Z\delta U + (f + Z)\ D\ . \tag{4.7}$$

Results of computing these accelerations appear in Tables 10 and 11. Two values are given for $\dot{D}$ and $\dot{D}^*$, corresponding to storm velocities of 330° 9 kt and 330° 6 kt. It is difficult to attach much importance to the differences shown between the two values of $\dot{D}$ or $\dot{D}^*$.

It is more interesting to compare $\dot{U}_0$ and $\dot{V}_0$ with the observed mean acceleration of Betsy given in Table 2. The direction of the storm acceleration is 150 degrees. The direction of the unbalanced force given by $\dot{U}_0$ and $\dot{V}_0$ varies from 148 to 152 degrees if the data at 12.5 km is excluded so that the force is essentially colinear with the mean storm acceleration. The magnitude of the unbalanced force is larger than the observed acceleration. The geopotential analysis is derived from data observed between 1830 and 2330 GMT and the wind analysis from data at 1650 to 2330 GMT. The geopotential is most important in giving $\dot{U}_0$ and $\dot{V}_0$, so it seems reasonable to adopt the storm acceleration observed between 1801 and 2110 GMT as the most appropriate to compare to the unbalanced force given here. Thus, the unbalanced force is between five and six times greater than the acceleration. If the mean acceleration from 1601 to 2110 GMT is compared, the unbalanced force is nearly four times larger than this acceleration.

Since $\dot{U}_0$ and $\dot{V}_0$ are obtained from the average geopotential from 1830 to 2330 GMT, it would be logical to inquire whether these accelerations are observed. Changes in the wind of the order of 5 m sec^{-1} may be expected in 3 hr and should be detectable. In Chapter V, the observed acceleration of the wind field is examined at nineteen points with the conclusion that the accelerations given by (4.4) and (4.5) may not occur. Next, in Chapter VI, the relation between the unbalanced geopotential force of (4.4) and (4.5) and the storm acceleration is investigated. It is hypothesized that the observed mean tropical storm acceleration is given by this force. As a part of this hypothesis, the acceleration of the basic current is also related to the unbalanced geopotential force.

CHAPTER V

ACCELERATION OF THE OBSERVED WIND

Data to compute the acceleration of the wind field in a coordinate system moving with the center of the tropical storm are given in Table 12 for nineteen points where the aircraft flight paths cross or come close together. Fig. 1 shows the flight path with each of these points identified by number. D[illegible]2 are the location of the observations given by angl[illegible]ise from east as zero and distance from the st[illegible]eters, the time of the first wind observat[illegible]n observations in hours, the wind directi[illegible]coordinates (north wind zero, east 90 degree[illegible] for both observations. The average wind ac[illegible]propriate time interval appears in Table 13 where the wind [illegible]ved into u(east) and v(north) components and the acceleration is given for each component in units of 10^{-4}m sec^{-2}.

The observed accelerations may be classified with respect to typical accelerations which may be expected based on elementary scale analysis. Length scales which pertain to hurricane accelerations are the diameter of the maximum wind belt, ≈ 100 km, the diameter of the cyclonic circulation, ≈ 1000 km, and the depth of the storm, ≈ 10 km. Velocity scales corresponding to these length scales are the maximum

CHAPTER V

ACCELERATION OF THE OBSERVED WIND

Data to compute the acceleration of the wind field in a coordinate system moving with the center of the tropical storm are given in Table 12 for nineteen points where the aircraft flight paths cross or come close together. Fig. 1 shows the flight path with each of these points identified by number. Data in Table 12 are the location of the observations given by angle measured counterclockwise from east as zero and distance from the storm center measured in kilometers, the time of the first wind observations, the time interval between observations in hours, the wind direction measured in meteorological coordinates (north wind zero, east 90 degrees, etc.,), and speed in kts for both observations. The average wind acceleration over the appropriate time interval appears in Table 13 where the wind is resolved into u(east) and v(north) components and the acceleration is given for each component in units of 10^{-4}m sec^{-2}.

The observed accelerations may be classified with respect to typical accelerations which may be expected based on elementary scale analysis. Length scales which pertain to hurricane accelerations are the diameter of the maximum wind belt, ≈ 100 km, the diameter of the cyclonic circulation, ≈ 1000 km, and the depth of the storm, ≈ 10 km. Velocity scales corresponding to these length scales are the maximum wind, $\approx$ 50m sec^{-1}, the wind near the edge of the cyclonic circulation, $\approx$ 10 m sec^{-1}, and the maximum updraft speed in cumulus clouds, $\approx$ 5 m sec^{-1}.

Time scales corresponding to the above are given by

2×10^3 sec	for maximum wind
10^5 sec	at the edge of cyclonic circulation

and

2×10^3 sec	in the convection area .

The synoptic time scale in the tropics was given above as 10^5 sec. The convection scale refers to the deep cumulus convection which is observed in the area of the maximum wind. Not unexpectedly, the time scale for the maximum wind corresponds to the convective scale because these winds are generated by the horizontal pressure gradient (here geopotential), induced by warming of the middle and high troposphere caused primarily by release of latent heat in the cumulus convection. This is the essential mechanism to generate and maintain the hurricane. The scale for the cyclonic circulation was computed near the edge of the circulation so that it is reasonable that it correspond to the synoptic scale. In the hurricane, time scales range continuously between the shortest and longest. It may be meaningful to define three time scales,

2×10^3 sec	for Convective,
10^4 sec	for Hurricane,

and

10^5 sec	for Synoptic .

The convective scale describes events near the radius of maximum winds, the hurricane scale is typical of the region between the maximum wind area and the outside of the storm, and the synoptic scale corresponds to the edge of the storm and the synoptic changes outside the storm. The time scales given agree with those used by Sasaki and Syono (1968) in a formal scale analysis of (2.56) and (2.57).

Typical accelerations in each of these areas are

Convective	250×10^{-4} m sec^{-2},
Hurricane	20×10^{-4} m sec^{-2},
and Synoptic	1×10^{-4} m sec^{-2}.

These accelerations are representative of a typical hurricane occurrance. For the tropical storm Betsy, the appropriate wind scales are 20 m sec^{-1} in the convective region and 10 m sec^{-1} in the hurricane region, which give accelerations

Convective (Betsy)	40×10^{-4} m sec^{-2}
and Hurricane (Betsy)	5×10^{-4} m sec^{-2}.

One observation in Table 12 at 172° 27.5 km clearly belongs to the convective accelerations, both in time interval and acceleration observation. The point at 185° 60 km has a time interval short enough to observe convection changes also, and the observed acceleration lies between the convective and hurricane scales and probably belongs to the former. The remaining accelerations belong to the hurricane scale by virtue of their occurrance in the cyclonic circulation, even though some have the magnitude of synoptic accelerations.

It is useful to ask whether the observed wind accelerations agree with the acceleration data from the Sasaki-Syono model. The model gives the acceleration of the wind in the moving coordinate, but as viewed from the fixed frame, as

$$\dot{u} + \ddot{X} = \dot{U}_0 - \dot{v}_{\theta 0} \sin\theta + \dot{D} \cos 2\theta + \dot{D}^* \sin 2\theta \qquad (5.1)$$

and

$$\dot{v} + \ddot{Y} = \dot{V}_0 + \dot{v}_{\theta 0} \cos\theta + \dot{D} \sin 2\theta - \dot{D}^* \cos 2\theta \ . \qquad (5.2)$$

The average symmetric acceleration, $\dot{v}_{\theta 0}$, was estimated by taking the average of the nineteen points to be 5.23×10^{-4} m sec^{-2}. If the two points reflecting convective scale accelerations are excluded, $\dot{v}_{\theta 0}$ = 2.66×10^{-4} m sec^{-2}, and the latter figure would be more representative of the hurricane scale data which is of interest here. To compare (5.1) and (5.2) with the observed accelerations, assume the accelerations of (5.1) and (5.2) are uniform over the time interval of the observations and use them to calculate the wind at the end of the time periods which may be compared to the corresponding observed wind. This comparison is facilitated by computing the root-mean-square vector error (RMSVE) of the wind and comparing this with the root-mean-square vector displacement (RMSVD) which measures the observed wind change. This computation was done using average values of $\dot{D}$ and $\dot{D}^*$ from the storm movements of 330° 9 kt and 330° 6 kt. The results for the seventeen hurricane scale points give RMSVE = 11.0 m sec^{-1} and RMSVD = 6.29 m sec^{-1}. Agreement between (5.1) and (5.2) and the observed accelerations is not found because the error vector is much larger than the displacement vector.

Two criticisms of this computation are apparent. First, the observed wind changes include all harmonics of the wind and (5.1) and (5.2) contain the zero and first harmonic. Second, (4.4) to (4.7) may be integrated if φ_1 and φ_1^* are held fixed and this may give a different result. Nothing can be done about the first point. A computation described below shows that integration of (4.4) to (4.7) would be unlikely to reduce the error vector below the displacement vector.

An approach to understanding the acceleration of the wind field of the hurricane which gives an error vector RMSVE = 3.48 m sec^{-1}, compared to the displacement vector RMSVD = 6.29 m sec^{-1}, is described below. The change of the wind field in the hurricane is predicted by assuming that the wind is approaching a state of balance between wind and pressure or mass (here geopotential). The balanced state turns out to be controlled by the symmetric geopotential φ_0, and to a small degree by the non-symmetric geopotential, φ_1 and φ_1^*. It was shown in Chapter IV that the first harmonic of the wind and geopotential are not in a state of balance or equilibrium. A similar condition occurs with respect to φ_0, as evidenced by the $\dot{v}_{\theta 0}$ given above and the deepening of the central pressure of the storm mentioned in Chapter III.

Since the wind and geopotential are observed not to be in a balanced state, it is meaningful to ask whether the wind field, whose changes at nineteen points are known, is approaching toward equilibrium given by the geopotential field. It may be noted that the approach to the hurricane wind change given here differs from Chapter II where the wind and its acceleration are assumed and the geopotential to balance it is computed. Here, the geopotential is to be more fundamental, and the difficult problem of inferring the response of the wind field to the given geopotential is considered. Because (2.1) is nonlinear in the wind field, this approach must be approximate as opposed to the exact discussion of Chapter II.

The simplest and most extensively studied expressions of equilibrium are the geostrophic wind equations. To illustrate, (2.1) may be written neglecting surface friction as

$$\frac{du}{dt} + \ddot{X} - f(v + \dot{Y}) = - \frac{\partial\varphi}{\partial x} \tag{5.3}$$

and

$$\frac{dv}{dt} + \ddot{Y} + f(u + \dot{X}) = - \frac{\partial\varphi}{\partial y} \tag{5.4}$$

where

$$\frac{d}{dt} = \frac{\partial}{\partial t} + u \frac{\partial}{\partial x} + v \frac{\partial}{\partial y} \tag{5.5}$$

which is often referred to as the total or substantial derivative and denotes differentiation following a fluid parcel in the Lagrangian sense. Geostrophic balance is the statement that the Lagrangian acceleration vanishes and the geostrophic wind equations in the moving coordinates are

$$u + \dot{X} = - \frac{1}{f} \frac{\partial\varphi}{\partial y} \tag{5.6}$$

and

$$v + \dot{Y} = \frac{1}{f} \frac{\partial\varphi}{\partial x} . \tag{5.7}$$

Eqs (5.6) and (5.7) can be exactly satisfied only for straight contours of φ and the corresponding linear current. It is well known, however, that the large-scale atmospheric wind systems, outside the tropics where the Coriolis parameter is too small, are continuously in a state of quasi-geostrophic balance (Charney 1948). This fact has important practical consequences because it is much easier to describe and predict equilibrium states than to deal with the full complexity of motions which are possible in the atmosphere (Charney 1949). Much of theoretical meteorology and numerical forecasting theory are founded upon this concept.

The approach of the mass and wind fields toward equilibrium is known as the adjustment problem and was first discussed by Rossby (1938). Rossby considered the geostrophic adjustment of a linear current along the x axis in a homogeneous incompressible ocean of uniform depth ($\nabla\varphi = 0$). Initially, the current is accelerated toward the right (looking downstream) by the Coriolis force, resulting in piling up of fluid on that side of the current and a depression on the left. This produces the geopotential distribution to balance the current. But, because of the inertia of the fluid, the current overshoots the equilibrium position and begins to oscillate with a frequency a little less than f (Cahn 1945). The oscillation is damped by propagation of energy away from the current by gravity waves and equilibrium ensues. After just a few oscillations, the current is very near equilibrium and a reasonable approximation to balance occurs in the first oscillation. The oscillation period is near 30 hours at 20°N.

Approach to equilibrium in a tropical storm or hurricane is significantly different from the linear current problem due to rotation because the current oscillation frequency is approximately given by $f + Z$ rather than f, and this reduces the period to about 6 hours for the data of Betsy. This results in quicker adjustment and, according to our results below, to dominance of the φ_0 geopotential over φ_1 and φ_1^*.

In the atmosphere the mass field is not controlled exclusively by the wind or momentum field, but it is controlled primarily by the temperature field which is controlled by heat sources and sinks and the momentum field. Equilibrium is most unlikely to occur, but the quasi-balanced motions in the atmosphere proceed through a series of quasi-equilibrium states, and the corresponding wind changes are the superposition of the change of equilibrium state plus gravity-inertia oscillations. The accelerations of the latter are larger than the former and far more difficult to compute. Changes of equilibrium states are often induced by unstable distributions of mass or momentum in the atmosphere which may result in large accelerations. An example are the accelerations in the convective region of the hurricane noted above. The change of φ_0 in the hurricane is controlled primarily by latent heat release in convection. The fact that φ_0 is controlled by heating and may thus change independent of the wind field is probably the reason that mean geopotential values can predict changes of the wind occurring during the collection of data. The nature of the unbalanced φ_1 and φ_1^* fields will be discussed in Chapter VI.

To discuss the balance of wind with the symmetric geopotential, it is necessary to write (2.1) in moving polar coordinates. Thus

$$\frac{\partial v_r}{\partial t} + \ddot{R} + v_r \frac{\partial v_r}{\partial r} + \frac{v_\theta}{r}\frac{\partial v_r}{\partial \theta} - \frac{v_\theta^2}{r} - f(v_\theta + R\dot{\theta}) = -\frac{\partial \varphi}{\partial r} \qquad (5.8)$$

and

$$\frac{\partial v_\theta}{\partial t} + R\ddot{\theta} + v_r \frac{\partial v_\theta}{\partial r} + \frac{v_\theta}{r}\frac{\partial v_\theta}{\partial \theta} + \frac{v_r v_\theta}{r} + f(v_r + \dot{R}) = -\frac{1}{r}\frac{\partial \varphi}{\partial \theta} \tag{5.9}$$

where

$$\dot{R} = \dot{X}\cos\theta + \dot{Y}\sin\theta \text{ and } R\dot{\theta} = -\dot{X}\sin\theta + \dot{Y}\cos\theta \tag{5.10}$$

and $\ddot{R}$ and $R\ddot{\theta}$ are similarly defined with respect to $\ddot{X}$ and $\ddot{Y}$. Equilibrium in the Lagrangian sense cannot occur, but equilibrium in the Eulerian time derivative is possible when $\varphi = \varphi_0$. If the geopotential contours are stationary and f taken to be constant, the equilibrium solution is

$$\frac{v_\theta^2}{r} + f\,v_\theta = \frac{\partial \varphi_0}{\partial r} \tag{5.11}$$

and (5.11) is known as the gradient wind equation. The equilibrium given by (5.11) can also exist in a moving coordinate system provided an asymmetric geopotential φ_a is given where

$$\varphi_a = \varphi_1 \cos\theta + \varphi_1^* \sin\theta\ . \tag{5.12}$$

If the symmetric geopotential contours translate with a uniform velocity, (5.11) is the equilibrium solution if

$$fR\dot{\theta} = \frac{\partial \varphi_a}{\partial r} \tag{5.13}$$

and

$$f\dot{R} = -\frac{1}{r}\frac{\partial \varphi_a}{\partial \theta} \tag{5.14}$$

or, in rectangular coordinates

$$U_0 = \dot{X} = -\frac{1}{f}\frac{\partial\varphi_a}{\partial y} \tag{5.15}$$

and

$$V_0 = \dot{Y} = \frac{1}{f}\frac{\partial\varphi_a}{\partial x} \quad . \tag{5.16}$$

If the φ_0 contours accelerate, the equilibrium is given by (5.11) and the conditions

$$\dot{U}_0 = \ddot{X} = f\,\dot{Y} - \frac{\partial\varphi_a}{\partial x} \tag{5.17}$$

and

$$\dot{V}_0 = \ddot{Y} = -\,f\,\dot{X} - \frac{\partial\varphi_a}{\partial y} \tag{5.18}$$

and (5.17) and (5.18) mean that the vortex is accelerating with the basic current.

Eqs. (5.11), (5.17) and (5.18) describe a possible state of equilibrium between the symmetric wind and geopotential of a vortex in which the unbalanced φ_a gives the acceleration of the vortex and basic current. The vortex acceleration is given because v_r is required to vanish. That this equilibrium state is not the equilibrium state which governs tropical storms and hurricanes is evident because the observed $\ddot{X}$ and $\ddot{Y}$ do not agree with (5.17) and (5.18), as is clearly shown in Tables 9 and 10. This is important because the results below show that (5.11) is a reasonable approximation to the balance of the symmetric wind and the geopotential so that it is the problem of φ_a which needs further discussion. A clue to the discussion is the existence of v_r and a basic current in the moving coordinate, which have been ignored in the discussion so far.

It is convenient to work with the cartesian form of (2.1) but with the non-linear terms expressed in polar form. Thus

$$u\frac{\partial u}{\partial x} + v\frac{\partial u}{\partial y} = v_r\frac{\partial v_r}{\partial r}\cos\theta - v_r\frac{\partial v_\theta}{\partial r}\sin\theta$$

$$- \frac{v_\theta v_r}{r}\sin\theta - \frac{v_\theta{}^2}{r}\cos\theta + \frac{v_\theta}{r}\frac{\partial v_r}{\partial\theta}\cos\theta - \frac{v_\theta}{r}\frac{\partial v_\theta}{\partial\theta}\sin\theta \qquad (5.19)$$

and

$$u\frac{\partial v}{\partial x} + v\frac{\partial v}{\partial y} = v_r\frac{\partial v_r}{\partial r}\sin\theta + v_r\frac{\partial v_\theta}{\partial r}\cos\theta$$

$$+ \frac{v_\theta v_r}{r}\cos\theta - \frac{v_\theta{}^2}{r}\sin\theta + \frac{v_\theta}{r}\frac{\partial v_r}{\partial\theta}\sin\theta + \frac{v_\theta}{r}\frac{\partial v_\theta}{\partial\theta}\cos\theta\ . \qquad (5.20)$$

The principal components of the geopotential which are to be considered are the symmetric and the uniform gradient. The principal wind fields related to these geopotential components are the symmetric wind and the basic current. The basic current in the moving coordinate is given by δU_0 and δV_0. It is desired to retain the terms of (5.19) and (5.20) which describe the basic current plus the symmetric wind. By noting that

$$v_r = u\cos\theta + v\sin\theta\ , \qquad (5.21)$$

$$v_\theta = -\,u\sin\theta + v\cos\theta\ , \qquad (5.22)$$

$$u = v_r\cos\theta - v_\theta\sin\theta\ , \qquad (5.23)$$

and

$$v = v_r \sin\theta + v_\theta \cos\theta \, , \tag{5.24}$$

(5.19) and (5.20) may be written for the symmetric wind and basic current as

$$u\frac{\partial u}{\partial x} + v\frac{\partial u}{\partial y} = -\frac{v_\theta}{r} v + \frac{v_\theta}{r}\delta V_0 - v_r \frac{\partial v_\theta}{\partial r}\sin\theta \tag{5.25}$$

and

$$u\frac{\partial v}{\partial x} + v\frac{\partial v}{\partial y} = \frac{v_\theta}{r} u - \frac{v_\theta}{r}\delta U_0 + v_r \frac{\partial v_\theta}{\partial r}\cos\theta \, . \tag{5.26}$$

Note that if $u = \delta U_0$ and $v = \delta V_0$ that (5.25) and (5.26) vanish, as they must for a linear current. With (5.25) and (5.26), (5.3) and (5.4) may be written in a form to consider the balance with the φ_0 and φ_a geopotential as

$$\dot{u} + \ddot{X} - \frac{v_\theta}{r} v + \frac{v_\theta}{r}\delta V_0 - v_r \frac{\partial v_\theta}{\partial r}\sin\theta - f(v + \dot{Y}) = -\frac{\partial}{\partial x}(\varphi_0 + \varphi_a) \tag{5.27}$$

and

$$\dot{v} + \ddot{Y} + \frac{v_\theta}{r} u - \frac{v_\theta}{r}\delta U_0 + v_r \frac{\partial v_\theta}{\partial r}\cos\theta + f(u + \dot{X}) = -\frac{\partial}{\partial y}(\varphi_0 + \varphi_a) \, . \tag{5.28}$$

Eqs. (5.27) and (5.28) are non-linear, there are three unknowns, the basic current components and the symmetric wind speed, and the radial derivative of v_θ is required. To obtain a simple approximate balance solution, let us impose the condition that one possible balance state be given by (5.11) plus (5.6) and (5.7), or the sum of the gradient and geostrophic wind. Let the geopotential be expressed with the aid of

(5.11), (5.6) and (5.7) as

$$-\frac{\partial}{\partial x}(\varphi_0+\varphi_a) = -\left(\frac{v_{\theta\,gr}}{r}+f\right) v_{gr} - f\,v_{geo} \tag{5.29}$$

and

$$-\frac{\partial}{\partial y}(\varphi_0+\varphi_a) = \left(\frac{v_{\theta\,gr}}{r}+f\right) u_{gr} + f\,u_{geo} \tag{5.30}$$

for the sum of a symmetric and uniform gradient geopotential. The subscript "gr" denotes the gradient wind and "geo" denotes the geostrophic wind which balances the symmetric and linear geopotential, respectively. Let

$$u = u_0 + \delta U_0 \quad \text{and} \quad v = v_0 + \delta V_0 \tag{5.31}$$

where the u_0 and v_0 are the symmetric components of u and v. Substitute (5.29) to (5.31) into (5.27) and (5.28) with $\dot{u} + \ddot{X} = \dot{v} + \ddot{Y} = 0$ to seek a balanced state to obtain

$$\left(\frac{v_\theta}{r}+f\right)v_0 + \left(\frac{v_\theta}{r}+f\right)\delta V_0 - \frac{v_\theta}{r}\delta V_0 + f\dot{Y} + v_r\frac{\partial v_\theta}{\partial r}\sin\theta =$$

$$\left(\frac{v_{\theta\,gr}}{r}+f\right) v_{gr} + f\,v_{geo} \tag{5.32}$$

and

$$\left(\frac{v_\theta}{r}+f\right)u_0 + \left(\frac{v_\theta}{r}+f\right)\delta U_0 - \frac{v_\theta}{r}\delta U_0 + f\dot{X} + v_r\frac{\partial v_\theta}{\partial r}\cos\theta =$$

$$\left(\frac{v_{\theta\,gr}}{r}+f\right) u_{gr} + f\,u_{geo}\,. \tag{5.33}$$

If the terms of $\partial v_\theta/\partial r$ are neglected, (5.32) and (5.33) have as one solution $v_\theta = v_{\theta\,gr}$, $u_0 = u_{gr}$, $v_0 = v_{gr}$, $U_0 = u_{geo}$, and $V_0 = v_{geo}$. Retention of these terms would require addition of wind and/or geopotential components in addition to the symmetric and linear terms being considered; as the problem is already complicated, this step is not attempted here. Mean values of these terms were computed using the observed δU_0, δV_0 and v_θ and found not to significantly alter the results given below, neglecting the $\partial v_\theta/\partial r$ terms. Discussion of (5.32) and (5.33) is facilitated if these equations are linearized. This may be done by setting $v_\theta = v_{\theta\,gr}$ in the first three terms of each equation, and the elementary solution given above still holds. And transferring the result to (5.27) and (5.28) gives

$$\dot{u} + \ddot{X} - F(v + \dot{Y}) + Z_{gr}V_0 = -\frac{\partial}{\partial x}(\varphi_0 + \varphi_a) \tag{5.34}$$

and

$$\dot{v} + \ddot{Y} + F(u + \dot{X}) - Z_{gr}U_0 = -\frac{\partial}{\partial y}(\varphi_0 + \varphi_a) \tag{5.35}$$

where $F = Z_{gr} + f$ and $Z_{gr} = v_{\theta\,gr}/r$. Eqs. (5.34) and (5.35) are very convenient because the wind and acceleration appear as they are measured with respect to the fixed coordinate system, although they must be computed at points in the moving coordinates.

Eqs. (5.34) and (5.35) have three unknown quantities if the wind is restricted to the sum of the symmetric and linear components. If this condition is relaxed, there are four unknowns, two of which must be given in order to find solutions. Since these equations must interpret data which is unconstrained, the latter posture is taken. This leaves little choice but to specify U_0 and V_0, the basic current in the fixed coordinate. This is a fortunate circumstance because the observed values of U_0 and V_0 in Table 5, which may be used in (5.34) and (5.35), are an order of magnitude less than the velocity components observed in Table 13, so that the Z_{gr} terms will be an order less than the F terms. Coincident with the expanded interpretation of u and v above, the non-symmetric geopotential φ_a will be given by (5.12) and not restricted to the linear portion of φ_a , as implied in the discussion of (5.29) and (5.30) but, for convenience, the form of (5.29) and (5.30) is adopted.

The equilibrium or balanced solutions of (5.34) and (5.35) are given by

$$u + \dot{X} = u_{gr} + \frac{f}{F} u_{geo} + \frac{Z_{gr}}{F} U_0 \tag{5.36}$$

and

$$v + \dot{Y} = v_{gr} + \frac{f}{F} v_{geo} + \frac{Z_{gr}}{F} V_0 \ . \tag{5.37}$$

The time dependent solutions, assuming φ_0 and φ_a are stationary, are

$$u + \dot{X} = \alpha_1 \cos Ft + \beta_1 \sin Ft + u_{gr} + \frac{f}{F} u_{geo} + \frac{Z_{gr}}{F} U_0 \tag{5.38}$$

and

$$v + \dot{Y} = \alpha_2 \cos Ft + \beta_2 \sin Ft + v_{gr} + \frac{f}{F} v_{geo} + \frac{Z_{gr}}{F} V_0 \tag{5.39}$$

where

$$\alpha_1 = (u + \dot{X})_i - (u_{gr} + \frac{f}{F} u_{geo} + \frac{Z_{gr}}{F} U_0), \tag{5.40}$$

$$\beta_1 = (\dot{u} + \ddot{X})_i \ , \tag{5.41}$$

and

$$\alpha_1 = - \beta_2 \quad \text{and} \quad \alpha_2 = \beta_1 \ . \tag{5.42}$$

The subscript "i" denotes the initial value of the quantity in brackets. The time dependent solutions can only be useful for periods short enough that time variations of φ_0 and φ_a are unimportant.

The form of the equilibrium solutions reveals the prime importance of the gradient wind with respect to the geostrophic wind. The factor f/F is about 1/5. Only if the basic current equals the geostrophic wind does this wind appear in equal status with the gradient wind. This is the important difference between the equilibrium conditions (5.36) and (5.37) and the model of Chapter IV, where a large acceleration of the basic current is required if there is no geostrophic balance with the linear geopotential. Here it is possible to examine the quasi-balance wind changes without committing ourselves to a basic current acceleration or geostrophic balance.

The observed basic current at 125 km was used together with φ_0, φ_1 and φ_1^* to compute (5.36) and (5.37). The symmetric geopotential φ_0, together with the gradient wind $v_{\theta\,gr}$ and Z_{gr}, are given in Table 14. The equilibrium solutions are given in Table 15 along with u_{gr}, v_{gr}, u_{geo} and v_{geo}. The error vector for predicting the acceleration of the observed wind, assuming its approach to the equilibrium given by (5.36) and (5.37), is obtained from the square root of the mean variance between the equilibrium solutions in Table 15 and the observed wind components of

Table 13. The result for the seventeen hurricane scale points was RMSVE = 3.48 m sec^{-1} and thus compares to the RMSVD = 6.29 m sec^{-1}. If all nineteen points are included, RMSVE = 4.76 m sec^{-1} and RMSVD = 6.9 m sec^{-1}, the latter error being 69% compared to the former 55% as would be expected because (5.36) and (5.37) may not apply to convective scale wind changes. Two other estimates of the wind change may be interesting. If the gradient wind is used to predict the wind change, the result is RMSVE = 3.79 m sec^{-1}. If the sum of the gradient and geostrophic wind is used to predict the wind change, the result is RMSVE = 11.18 m sec^{-1}. The last two statistics are computed at seventeen points. These results show the dominance of the gradient wind and the symmetric unbalanced geopotential on the wind field changes. At least in the time intervals considered here, no approach toward gradient-geostrophic equilibrium is apparent. On the other hand, the gradient wind alone is nearly as good a predictor as (5.36) and (5.37) and it may be appropriate to call the balance observed here quasi-gradient equilibrium. The latter result is because the basic current is small in this case. The lack of balance of the average symmetric wind with respect to the symmetric geopotential is shown by comparing the gradient wind of Table 14 to the observed $v_{\theta 0}$ in Table 7. The average observed $\dot{v}_{\theta 0} = 2.66 \times 10^{-4}$ m sec^{-2}, which is near 2.8 m sec^{-1} $(3\ hr)^{-1}$.

The time dependent solutions (5.38) and (5.39) show an inertia oscillation about the balanced solution of (5.36) and (5.37). This is an undamped oscillation. If the geopotential was allowed to vary, Cahn's results imply that the oscillation frequency would decrease a little and the oscillation would be damped toward zero by propagation of energy toward infinity by gravity waves. It was noted above that the frequency of the current oscillations during adjustment in a rotating wind system are greater than the non-rotating wind case. This result follows from (5.38) and (5.39) where the frequency is F, which is nearly five times larger than f in our data.

The solutions of (5.38) and (5.39) were computed at each of nineteen points, assuming the basic current for 125 km from Table 4. The RMSVE = 7.98 m sec^{-1} at nineteen points and 7.65 m sec^{-1} at the seventeen hurricane scale points. Since the error vector is larger than the displacement vector, this method of estimating the acceleration does not work. Above, it was noted in the discussion of (5.1) and (5.2) that solution of these equations by integration of (4.4) to (4.7) may not give a satisfactory result. The computation here is similar to that computation, and the conclusion follows from the results here.

Eqs. (5.38) and (5.39) predict the existence of inertia oscillations whose period is near 6 hours. These oscillations cannot be detected in the mean wind or geopotential data but may appear in the wind acceleration data. Attention is called to the observations in Table 12 in the west quadrant of the storm between 150° and 230° excepting the observation at 27.5 km. Note that, during the time interval between 2000 and 2300 GMT, the wind changes direction in the clockwise sense at all points, the changes being about 15 to 20 degrees. Two pairs of observations span a much shorter time interval, one near 2000 GMT (205°/120 km), the other near 2300 GMT (185°/60 km). Note that these two observations show counter-clockwise turning of the winds at these two points. It may be reasonable to assume that the first of these observation pairs occurred near the end of one phase of an inertia oscillation and that the second occurred at the beginning of the same phase a little more than half a period later and that the observations spanning 2000 to 2300 GMT refer to the opposite phase of the oscillation. This would give a period near 6 hours. The average values for F for these points is $2.6 \times 10^{-4} \sec^{-1}$ which gives a period of 6.71 hours.

With an inertia oscillation evident in the west quadrant of the storm, it may be appropriate to question why the wind given by (5.38) and (5.39) does not give a better result. In addition to the list of approximations which lead to these equations, two problems exist, even if (5.38) and (5.39) correctly describe the wind changes for short time periods. First, it is difficult to expect average wind and geopotential values to give the correct initial conditions to match the observed wind at each of seventeen points and, second, even with reasonable initial conditions, oscillations which have argument Ft beyond the first quadrant (this includes most of the points) are unlikely to give reasonable results because mutual adjustment of wind and geopotential becomes important in less than half a period. There is a pair of wind observations at $120^{\circ}/105$ km taken at 2000 and 2058 GMT which are not included in the results above. Since this point lies in the hurricane region, argument Ft is 38°, and the inertia oscillation occurs at this point, the solution may be interesting. It is

$$u + \dot{X} = - .75 \cos Ft + 10.44 \sin Ft + 4.90 = 10.76 \text{ m sec}^{-1} \quad (5.43)$$

and

$$v + \dot{Y} = 10.44 \cos Ft + .75 \sin Ft - 14.85 = - 6.20 \text{ m sec}^{-1}. \quad (5.44)$$

The prediction is over 100% in error, but the error is reduced to zero if $\alpha_1 = 2.13$ and $\beta_1 = 6.84$. Sensitivity of (5.38) and (5.39) to the values of α_1 and β_1 is evident here so that it is very optimistic to expect a good result.

It was noted above that the solution of (5.36) and (5.37) gives a 55% error vector for predicting the observed wind changes. Certainly the presence of an inertia oscillation, which is filtered out of the equilibrium calculations, may induce part of this error. It is also apparent from Tables 13 and 15 that the largest percentage errors occur where little change of the wind occurs and, in fact, many of the large changes agree much better than 50%. At points where small wind field changes are occurring, the presence of a convective cloud at one of the observation times could easily give a bad result. The large error at 030° 115 km can be reduced significantly if the profile of φ_1 in Fig. 6 is smoothed from 100 to 125 km. This also improves the result at 205° 120 km.

These points are cited to give additional support to the principle conclusions of this chapter. These are that the hurricane wind field is continuously evolving toward a quasi-equilibrium state, approximately given by (5.36) and (5.37), that the geopotential or mass fields leads the wind field, that the symmetric mode is dominant in the adjustment process, and that the adjustment occurs much quicker in a rotating than non-rotating wind system.

The role of the basic current and unbalanced linear geopotential in the computations above leaves some unanswered questions. Since the basic current was taken as a constant, the results suggest, but do not prove, that the acceleration of the basic current computed in Chapter IV may not occur during data collection. Also, the unbalanced linear geopotential plays a minor role in the equilibrium wind computations. In Chapter VI, a hypothesis is presented relating this unbalanced geopotential force and the acceleration of the basic current. The basic current acceleration is about 1/5 of the magnitude of this force so that taking the basic current to be an observed constant, compared to the change of the symmetric winds in the wind change computations above, may give a good result.

CHAPTER VI

ACCELERATION OF BETSY

In this chapter, the observed acceleration of Tropical Storm Betsy is discussed from two points of view, from inside and outside the storm. The data collected by the research aircraft covers the storm center out to a radius of 125 km, and these are used to discuss the acceleration of the core of the storm. Empirically, the mean acceleration of this storm as viewed from the interior is given by

$$\bar{\ddot{X}} = - K \frac{\partial \varphi_u}{\partial x} \tag{6.1}$$

and

$$\bar{\ddot{Y}} = - K \frac{\partial \varphi_u}{\partial y} \tag{6.2}$$

where φ_u is the mean unbalanced linear geopotential determined from the right hand sides of (4.4) and (4.5), respectively, and K has a mean value which is .18 between 1801 and 2110 GMT. Data are used at the 700 mb level to measure the environment steering current, and this is used to discuss the storm acceleration from the viewpoint of the interaction between the storm and its environment. Unfortunately, the data are insufficient to give a complete quantitative discussion of this subject, but it is important because some agreement between observation and theory is found, and it is hypothesized that the unbalanced geopotential force, which is accelerating the core of the storm, is induced by the interaction with the environment.

The equations of motion for a solid cylinder, which may be rotating, in a two dimensional flow field are obtained from

$$\pi R^2 \rho' [\ddot{X} - f\dot{Y} + \mu_1 \dot{X} + \mu_2 (\dot{X} - U)] = - \rho \int_0^{2\pi} \varphi \cos \theta R \, d\theta \qquad (6.3)$$

and

$$\pi R^2 \rho' [\ddot{Y} + f\dot{X} + \mu_1 \dot{Y} + \mu_2 (\dot{Y} - V)] = - \rho \int_0^{2\pi} \varphi \sin \theta R \, d\theta \qquad (6.4)$$

where ρ and ρ' are the fluid and cylinder densities, μ_1 and μ_2 the drag coefficients as discussed by Kuo (1969) for surface drag where the cylinder intersects the ocean or ground, and pressure drag resulting from eddy formation in the wake of the cylinder, respectively, and φ is evaluated at $r = R$, the radius of the cylinder. The boundary conditions at the cylinder are that V_{r1} and V_{r1}^* vanish. The appropriate equations for the geopotential are (2.44) and (2.45) and substitution into (6.3) and (6.4) gives

$$(1 + \frac{\rho'}{\rho}) \ddot{X} + [\zeta + 2Z + (1 - \frac{\rho'}{\rho}) f] \dot{Y} + [(\mu_1 + \mu_2) \frac{\rho'}{\rho} + \mu] \dot{X}$$

$$= 2\dot{U} + (2\mu + \mu_2 \frac{\rho'}{\rho}) U + (\zeta + 2Z) V \qquad (6.5)$$

and

$$(1 + \frac{\rho'}{\rho})\ddot{Y} - [\zeta + 2Z + (1 - \frac{\rho'}{\rho})f]\dot{X} + [(\mu_1 + \mu_2)\frac{\rho'}{\rho} + \mu]\dot{Y}$$

$$= 2\dot{V} + (2\mu + \mu_2\frac{\rho'}{\rho})V - (\zeta + 2Z)U \qquad (6.6)$$

where use has been made of (2.15), (2.16) and (2.37). Eqs. (6.5) and (6.6) are similar to Kuo's equations except for including the time variable steering current. They differ from Yeh's results by including drag terms, time variable steering current, and the influence of the Coriolis force on the cylinder or vortex is a small fraction of that on the surrounding fluid. It is noteworthy that the source m, which was introduced to complete (2.36), does not appear in (6.5) or (6.6). For application to an atmospheric vortex it is permissible to set $\rho = \rho'$ so that

$$\ddot{X} + \omega\dot{Y} + \alpha\dot{X} = \dot{U} + \alpha' U + \omega V \qquad (6.7)$$

and

$$\ddot{Y} - \omega\dot{X} + \alpha\dot{Y} = \dot{V} + \alpha' V - \omega U \qquad (6.8)$$

where $\omega = Z + \zeta/2$ is the angular velocity at the radius of the cylinder, $\alpha = \frac{1}{2}(\mu_1 + \mu_2 + \mu)$, and $\alpha' = \mu + \mu_2/2$.

The solution of (6.7) and (6.8) may be obtained for the case when the steering current is uniform in space or as $\zeta = 0$ and $\omega = Z$. Integrate each equation to obtain

$$\left(\frac{d}{dt} + \alpha \right) X + \omega Y = \dot{U}_0 t + \alpha' \int_0^t U_0 \, dt + \omega \int_0^t V_0 \, dt + C_1 \qquad (6.9)$$

and

$$\left(\frac{d}{dt} + \alpha \right) Y - \omega X = \dot{V}_0 t + \alpha' \int_0^t V_0 \, dt - \omega \int_0^t U_0 \, dt + C_2 \qquad (6.10)$$

where $U_0 = U_{00} + \dot{U}_0 t$ and $V_0 = V_{00} + \dot{V}_0 t$ and U_{00}, V_{00}, $\dot{U}_0$ and $\dot{V}_0$ are independent of time. The equations for X and Y are obtained by elimination and these equations are

$$\left(\frac{d}{dt} + \alpha \right)^2 X + \omega^2 X = K_1 + K_2 t + K_3 t^2 \qquad (6.11)$$

and

$$\left(\frac{d}{dt} + \alpha \right)^2 Y + \omega^2 Y = L_1 + L_2 t + L_3 t^2 \qquad (6.12)$$

where

$$K_1 = \alpha C_1 - \omega C_2 + \dot{U}_0 + \alpha' U_{00} + \omega V_{00}, \qquad (6.13)$$

$$K_2 = (\omega^2 + \alpha\alpha') U_{00} + \omega(\alpha - \alpha') V_{00} + (\alpha + \alpha') \dot{U}_0, \qquad (6.14)$$

$$K_3 = \frac{1}{2} [(\omega^2 + \alpha\alpha') \dot{U}_0 + \omega(\alpha - \alpha') \dot{V}_0], \qquad (6.15)$$

$$L_1 = \omega C_1 + \alpha C_2 + \dot{V}_0 - \omega U_{00} + \alpha' V_{00}, \qquad (6.16)$$

$$L_2 = (\omega^2 + \alpha\alpha') V_{00} + \omega(\alpha' - \alpha) U_{00} + (\alpha + \alpha') \dot{V}_0, \qquad (6.17)$$

and

$$L_3 = \frac{1}{2}[(\omega^2 + \alpha\alpha')\dot{V}_0 + \omega(\alpha' - \alpha)\dot{U}_0]. \tag{6.18}$$

The solutions of (6.11) and (6.12) are

$$X = Ae^{-\alpha t}\sin(\omega t + \epsilon) + \frac{1}{\omega^2+\alpha^2}[K_1 + K_2 t + K_3 t^2$$

$$- \frac{2\alpha K_2}{\omega^2+\alpha^2} - \frac{4\alpha K_3 t}{\omega^2+\alpha^2} - \frac{2K_3}{\omega^2+\alpha^2} + \frac{4\alpha^2 K_3}{(\omega^2+\alpha^2)^2}] \tag{6.19}$$

and

$$Y = Ae^{-\alpha t}\cos(\omega t + \epsilon) + \frac{1}{\omega^2+\alpha^2}[L_1 + L_2 t + L_3 t^2$$

$$- \frac{2\alpha L_2}{\omega^2+\alpha^2} - \frac{4\alpha L_3 t}{\omega^2+\alpha^2} - \frac{2L_3}{\omega^2+\alpha^2} + \frac{4\alpha^2 L_3}{(\omega^2+\alpha^2)^2}] \tag{6.20}$$

where A and ϵ can be expressed in terms of the remaining constants of the solution.

The trajectory given by (6.19) and (6.20) consists of two parts, a curved mean path which differs from the steering current due to the presence of drag forces plus an oscillation about the mean path. When the steering current is steady, the mean path is a straight line and the path including the oscillation is a damped trochoid. When acceleration of the steering current occurs, the mean path is a hyperbola which may degenerate to a straight line. The velocity components along the mean path are

$$\dot{\bar{X}} = \frac{\omega^2 + \alpha\alpha'}{\omega^2 + \alpha^2} U_0 + \frac{(\alpha - \alpha')\omega}{\omega^2 + \alpha^2} V_0$$

$$- \frac{(\omega^2 - \alpha^2)(\alpha - \alpha')}{(\omega^2 + \alpha^2)^2} \dot{U}_0 - \frac{\omega\alpha(\alpha - \alpha')}{(\omega^2 + \alpha^2)^2} \dot{V}_0 \tag{6.21}$$

and

$$\dot{\bar{Y}} = \frac{\omega^2 + \alpha\alpha'}{\omega^2 + \alpha^2} V_0 + \frac{(\alpha' - \alpha)\omega}{\omega^2 + \alpha^2} U_0$$

$$- \frac{(\omega^2 - \alpha^2)(\alpha - \alpha')}{(\omega^2 + \alpha^2)^2} \dot{V}_0 - \frac{\omega\alpha(\alpha' - \alpha)}{(\omega^2 + \alpha^2)^2} \dot{U}_0 \, . \tag{6.22}$$

When the steering current is steady, the angle between the steering current and the trajectory is given by

$$\tan\gamma = - \frac{(\alpha - \alpha')\omega}{\omega^2 + \alpha\alpha'} \tag{6.23}$$

as may be seen if the coordinate axes are rotated so that $V_0 = 0$. Since $\alpha - \alpha' = \frac{1}{2}(\mu_1 - \mu)$, it is apparent that $\gamma = 0$ when no drag forces are present, when there is pressure drag alone, or when the surface drag on the fluid in the cylinder is the same as the environment. The normal observed state indicates $\mu_1 > \mu$, so that the storm deviates to the right of the environment steering current when the vortex rotation is cyclonic ($\omega > 0$) and to the left for an anti-cylonic vortex ($\omega < 0$).

When the steering current is accelerating, further deviation of the path from the steering current than given by (6.23) may occur. According to Kuo, α is proportional to ω and may be of the same order of magnitude. Then, the added contributions to $\ddot{\bar{X}}$ and $\ddot{\bar{Y}}$ are approximately $\dot{U}_0/\omega$ and $\dot{V}_0/\omega$. Since $\dot{U}_0$ and $\dot{V}_0$ are of the order of 10^{-4}m sec^{-2} and ω is the order of 10^{-4}sec^{-1}, the added contributions to the mean velocity components are of the order of 1 m sec^{-1}. Note that the velocity of the storm lags the steering current velocity during acceleration as a result of the drag forces ($\mu_1 > \mu$).

The mean acceleration of the vortex may be obtained from (6.21) and (6.22) to be

$$\ddot{\bar{X}} = \frac{\omega^2 + \alpha\alpha'}{\omega^2 + \alpha^2} \dot{U}_0 + \frac{(\alpha - \alpha')\omega}{\omega^2 + \alpha^2} \dot{V}_0 \tag{6.24}$$

and

$$\ddot{\bar{Y}} = \frac{\omega^2 + \alpha\alpha'}{\omega^2 + \alpha^2} \dot{V}_0 + \frac{(\alpha' - \alpha)\omega}{\omega^2 + \alpha^2} \dot{U}_0 \tag{6.25}$$

The angle between the environment steering current acceleration and the storm acceleration is given by (6.23), and the magnitude of the storm acceleration is less than the magnitude of the steering current acceleration due to drag forces.

The model contained in (6.3) to (6.25) describes the interaction between a vortex and its environment following the approach of classical hydrodynamics. This theory does not apply to the interior of the vortex where the basic current may not agree with the environment steering current. For the aircraft data of Betsy, inside 125 km, this theory gives no explanation for the storm movement or acceleration failing to explain either the basic current or the unbalanced geopotential force.

Data to verify the theory of (6.3) to (6.25) must be acquired from that part of the storm where the basic current defined in Chapter III agrees with the environment steering current. This data does not exist in the aircraft reconnaissance flights for Betsy on the 29th of August 1965. The best that can be done is to examine the synoptic data and analyses for this data to determine the environment steering current. The data to do this were obtained from the Miami Hurricane Center. The available data leave much to be desired.

The steering current of tropical storm Betsy at 700 mb (10,000 ft) is estimated to be 120° 15 kt at 1200 GMT on 29 August. The estimate is based primarily upon two observations, a synoptic observation at Grand Truk, 480 mi ahead of the storm, and an aircraft observation, 900 mi behind the storm at 1750 GMT. The direction appears reliable to 5 degrees and the speed may be less but not as little as 10 kt. Data from 3000, 5000, and 14,000 feet suggest the 700 mb steering current may be typical of the whole layer from the ocean to 14,000 feet. At 500 mb (18,000 ft), a steering current cannot be readily defined but is less than 5 kt. At 300 mb (30,000 ft), the steering current is estimated from four wind observations to be 250° 10 kt. At 200 mb (40,000 ft), this current from the same stations is near 180° 10 kt. Little information on the depth of the storm at this time is known so that the relevance of the last two steering current estimates is in doubt. The storm definitely extends above 25,000 feet according to data at this level (400 mb), and there is weak evidence that the storm extends to 300 mb. It is interesting that the 300 mb current over the storm at 0000 GMT on 29 August was 120° 10 kt and that the presence of the storm may have been responsible for the change which occurred in the subsequent 12 hours.

To apply the two dimensional theory to Betsy where the observed steering current is not uniform with height requires an average steering current or the assertion that the storm movement is controlled by a particular layer of the atmosphere, in this case the layer from the surface to 14,000 feet. The appropriate way to define the mean steering current is unknown, but if account is taken of the strength of the storm circulation at each level, it is probable that the mean steering current is near 120° 15 kt at 1200 GMT on 29 August. The storm is moving toward 330° on the average between 1600 and 2300 GMT so that the storm may be moving 30 degrees to the right of the steering current and this agrees with the prediction of (6.23) for a cyclonic vortex. Kuo notes that if $\alpha \gg \alpha'$, then $\gamma = 25$ degrees when $\alpha = .446\ \omega$.

The steering current at 2400 GMT on 29 August or 0000 GMT on 30 August is very difficult to estimate because there are only two in place of the previous six synoptic network observations near the storm, and one of these is in the storm circulation. It appears from data at 700 mb, including four aircraft observations taken outside the storm, that the environment steering current has diminished below 10 kt and the direction is about 110 degrees. This is supported by a contour analysis by the Miami Hurricane Center. One station at 3000 and 5000 feet suggests that the current there may be near 120° 15 kt, although a smaller speed would be compatible because the station (Guadaloupe) is 300 mi southeast of the storm. At 500 mb, the steering current may be 120° 10 kt based upon this station. At 300 mb and 200 mb, the steering current is near 200° 15 kt, and a commercial airlines report at 200 mb aided this estimate. No further data on the depth of the storm is known. An appropriate mean current must be a guess and is taken here to be 115/10 kt. The important point is that evidence for a decrease in the speed of the environment steering current has been accepted. The steering current acceleration vector is near 120 degrees and the mean storm acceleration vector is near 150 degrees so that the latter is about 30 degrees to the right of the former, which is in agreement with (6.23).

Discussion of the relation between the track oscillation appearing in (6.19) and (6.20) and the observed track is difficult because ω is not known in that part of the storm where this theory may be valid. The period of oscillation from (6.19) is

$$\tau = 2\pi/\omega \ . \tag{6.26}$$

The data of Table 1 do not show the oscillation period, but if one is present, the period must be greater than 14 hours unless damping is sufficient to obscure a shorter period of oscillation. For example, when $\alpha = 0.5\,\omega$ and $\omega = 10^{-4}\text{sec}^{-1}$, the amplitude is reduced by 1/e in around 6 hours. The amplitude was not obtained above, but according to Yeh's results without drag forces, the amplitude is proportional to the difference between the storm velocity and the steering current velocity and inversely proportional to the period.

Syono (1955) proposed an alternative explanation of the track oscillation of a hurricane by relating it to an inertia oscillation of the steering current induced by the adjustment of wind and pressure. Syono used a steering model, but the same mechanism may enter (6.24) and (6.25) through $\dot{U}_0$ and $\dot{V}_0$ although the form of these solutions would change. The inertia period is about 30 hours at 20°N, so that the data of Table 1 could agree with an oscillation induced through the environment steering current acceleration.

A comment upon the nature of the interaction of the storm and its environment as given through $\dot{U}_0$ and $\dot{V}_0$ is appropriate. According to (2.44) and (2.45), this force upon the storm is a geopotential or pressure gradient force presuming that the gradient of the unbalanced geopotential is in the direction of the steering acceleration. But, as noted in Chapter V, the large-scale wind accelerations generally occur from one equilibrium state towards another in which the geopotential gradient associated with the wind change is perpendicular to rather than parallel to the wind change. In the tropics beyond 10 degrees from the equator, it is reasonable to assume that the $\dot{U}_0$ and $\dot{V}_0$ which control the mean acceleration components of the hurricane, $\ddot{\bar{X}}$ and $\ddot{\bar{Y}}$, are the result of adjustment of the wind to changes in the geopotential gradient perpendicular to $\dot{U}_0$ and $\dot{V}_0$, so that the interpretation of the force on the storm given by (2.44) and (2.45) may not apply. In the adjustment case, the force acting upon the storm is an inertia force. It is noteworthy that this force which occurs in the outer part of the storm and the storm acceleration are approximately equal, but according to (6.1) and (6.2), the storm acceleration is much less than the unbalanced linear geopotential force which is apparent in the interior of the storm. Below, a correspondence is hypothesized between this unbalanced geopotential force and a much smaller inertia force, the acceleration of the basic current inside the storm, which is hypothesized to induce the storm acceleration in the interior of the storm.

Before discussing our hypothesis, it may be noted that Sasaki and Syono (1968) give a theory for the mean acceleration of a hurricane which applies to the area of the storm where $Z \gg f$. When $Z \gg f$, (2.56) and (2.57) may be expanded in a small parameter ϵ, which is the ratio of the convective or maximum wind time scale to the time scale of f. The results of the expansion to the zero order in ϵ are

$$\frac{\tilde{\varphi}_1}{R} = - Z \left[2(\tilde{V}_0 - \tilde{\dot{Y}}_0) - \tilde{V}^*_{r1} \right] \qquad (6.27)$$

and

$$\frac{\tilde{\varphi}^*_1}{R} = Z \left[2(\tilde{U}_0 - \tilde{\dot{X}}) - \tilde{V}_{r1} \right] \qquad (6.28)$$

and to the first order

$$\epsilon \frac{\varphi_1'}{R} = \epsilon \, Z V^{*\prime}_{r1} - f[(\tilde{V}_0 - \tilde{\dot{Y}}) - \tilde{V}^*_{r1}] + f \tilde{V}_0 + \tilde{\dot{V}}_{r1} + \tilde{\ddot{X}} \qquad (6.29)$$

and

$$\epsilon \frac{\varphi^{*\prime}_1}{R} = - \epsilon \, Z V_{r1}' + f[(\tilde{U}_0 - \tilde{\dot{X}}) - \tilde{V}_{r1}] - f\tilde{U}_0 + \tilde{\dot{V}}^*_{r1} + \tilde{\ddot{Y}} \qquad (6.30)$$

where each parameter except Z, f and R has been expanded in series like

$$\varphi_1 = \tilde{\varphi}_1 + \epsilon\, \varphi_1{}' + \ldots . \tag{6.31}$$

$\dot{U}_0$ and $\dot{V}_0$ do not appear in (6.29) and (6.30) as they are assumed to be of higher order, but they may be added to these equations. φ_1 and φ_1^* correspond to the observed geopotential as do the other zero order terms in (6.27) and (6.28). The basic concept is to assume balance of the zero order Z terms to filter out this higher frequency from the acceleration of the vortex, which is obtained by introducing the quasi-solid assumption in which the boundary condition is

$$V_{r1}{}' = V_{r1}^{*}{}' = 0 \quad \text{at } r = R. \tag{6.32}$$

V_{r1} and V_{r1}^* do not vanish so that flow may occur across R in the moving coordinates. Substitution of (6.29) and (6.30) into (6.3) and (6.4), but with the drag forces omitted, gives

$$\ddot{X} = -\frac{f}{2} V_{r1}^{*} - \frac{1}{2} \dot{V}_{r1} + \dot{U}_0 \tag{6.33}$$

and

$$\ddot{Y} = \frac{f}{2} V_{r1} - \frac{1}{2} \dot{V}_{r1}^{*} + \dot{V}_0 \tag{6.34}$$

where ~ has been suppressed, $\rho = \rho'$, and the steering current acceleration has been included. Eqs. (6.33) and (6.34) may also be written

$$\ddot{X} = - f V_{r1}^{*} + \dot{U}_0 - \dot{D} \qquad (6.35)$$

and

$$\ddot{Y} = f V_{r1} + \dot{V}_0 - \dot{D}^{*} \qquad (6.36)$$

by use of (2.29) and (2.30).

The theory of Sasaki and Syono is difficult to apply to the aircraft data of Betsy because, although the assumption that $Z \gg f$ is fulfilled, the observed basic current does not agree with the environment steering current and the balance of wind and geopotential predicted by (6.27) and (6.28) is not observed, as may be seen from Tables 8 and 9. The average values, inside 125 km radius, of $V_{r1} = 5.5$ m sec^{-1} and $V_{r1}^{*} = -5.5$ m sec^{-1} from Table 3 and $f = .5 \times 10^{-4}$sec^{-1} so that the first terms on the right hand side of (6.35) and (6.36) are much larger terms than the observed mean storm acceleration components between 1601 and 2110 GMT, which were $\overline{\ddot{X}} = .69 \times 10^{-4}$m sec^{-2} and $\overline{\ddot{Y}} = -1.21 \times 10^{-4}$m sec^{-2}. Addition of the acceleration estimates from Tables 10 and 11 does not lead to a good result. The conclusion is that the Sasaki-Syono theory does not apply to these data. It would be difficult to apply this theory at radii larger than 125 km for this case because Z becomes of the same order as f.

The explanation of the observed mean acceleration of Tropical Storm Betsy in terms of the wind and geopotential data observed by aircraft within 125 km of the storm center has not been found in either the approach of Kuo or Sasaki and Syono. As pointed out above, an unbalanced uniform gradient geopotential force is observed inside 125 km. This force is several times larger than the acceleration of the storm but is essentially in the same direction. Two basic questions arise. First, what is the origin of the unbalanced geopotential φ_u? And second, why is $\nabla\varphi_u$ several times larger than the storm acceleration? A third area of inquiry involves the change in the storm acceleration rate asking whether this indicates a changing φ_u or a change in the storm's response to φ_u. Definitive answers cannot be given to any of these questions, but a set of hypotheses is offered below which may give a reasonable interpretation of the observations.

The origin of φ_u is hypothesized to be the result of interaction between the storm and its environment. It was noted above that, when time changes of the steering current are considered in Kuo's model, a force is exerted upon the storm at some radius which is not known at present but is certainly beyond 125 km in Betsy. According to (6.23), if the steering current acceleration is as presented above between 1200 and 2400 GMT, then a force should act on the storm approximately in the direction of the observed acceleration. The magnitude of the steering current acceleration appears to be consistent with the storm acceleration. This force may be an inertia force acting on the exterior of the storm circulation, but it would induce an unbalanced geopotential force inside the storm. The interior force should equal the force and acceleration of the exterior and is not expected to be several times larger.

Why is the geopotential force inside the storm several times larger than the acceleration of the storm or the exterior force? The approach to this problem given here is to consider a mechanism of storm acceleration inside 125 km and to show that the interior of the storm resists a force applied to the exterior. Note that this resistance is not the same as the virtual mass effect. The latter arises from the necessity of not only accelerating a mass of fluid, but also accelerating the escape motion which occurs when a fluid mass or object moves with a translation velocity different from its surroundings. In the present case, the surroundings or environment steering current are presumed to accelerate at a rate similar to the rotating fluid mass making up the storm interior so that a change of the escape motion is not required, or may be small compared to a case where the environment steering current does not accelerate.

The acceleration mechanism for the inside of the storm relates two differing scales of wind acceleration, one of the order of the observed hurricance acceleration (10^{-4}m sec^{-2}), the other of the order of the hurricane scale wind accelerations discussed in Chapter V (5×10^{-4}m sec^{-2}). The connection between these scales of acceleration is that discussed in the adjustment problem, where the acceleration of the wind through equilibrium states is much smaller than the instantaneous acceleration of the wind field, including gravity-inertia oscillations which are filtered out of the equilibrium calculations. In the present case, the unbalanced linear-geopotential force drives the gravity-inertia oscillations, and, through a physical process described below, generates a mean acceleration of air parcels approximately colinear with this force, but with the mean acceleration being much smaller than the force. The mean acceleration of parcels of air toward the southeast gives the storm acceleration inside 125 km and may be identified with the basic current acceleration, which may result in a basic current directed down the geopotential gradient. The observed basic current is directed toward 120 to 135 degrees with the speed near 3 kts. This agrees with the concept outlined here. Since the mean parcel accelerations down the geopotential gradient are less than this force, it is apparent that, in order to bring the acceleration of the exterior and interior of the storm into coincidence, it is necessary to have an interior force larger than the exterior acceleration. Here, we have proposed a hurricane acceleration mechanism that differs between the inside and outside of the storm and is related to the difference between the interior basic current and the environment steering current, which were first pointed out as evidence of an inside and outside of the storm.

The mechanism of the basic current acceleration inside 125 km is an adjustment problem controlled by the limited areal extent of the geopotential force inducing it and by the rotation of the storm interior. The limited areal extent of φ_u is the result of rotation resistance to the inertia force steering current acceleration acting on the exterior of the storm. Or, in other words, the rotation of the storm acts as a barrier which prevents changes of the environment steering current from penetrating to the interior of the storm. Steering current changes then must exert an inertia force on the exterior of the storm which is transmitted to the interior as an unbalanced geopotential force limited in areal exent. That is, it does not extend outside the storm.

To consider the basic current acceleration, first consider the response of an air parcel to φ_u, supposing no rotation and φ_u extends to infinity. Refer to Fig. 9 where the linear geopotential is shown in solid contours together with the direction of the basic current at 125 km and the storm acceleration. The geopotential which balances the Coriolis force of the basic current is shown by the dashed lines, and φ_u is the result of graphical subtraction of the dashed from the solid straight contours. Thus, the initial parcel acceleration is toward the southeast or near 150 degrees, but the parcel would be deflected toward the right or southwest by the Coriolis force, and an inertia oscillation of the current and φ_u geopotential would begin in the northwest-southeast direction as the air parcels proceed toward geostrophic equilibrium with φ_u in a southwesterly direction. The basic current would be toward the southwest in this case.

This is not observed and the reasons are the finite extent of φ_u and the rotation of the storm. First, note that assuming a quasi-gradient equilibrium initial condition that the deflecting force toward the southwest will be approximately proportional to F rather than f, due to the centrifugal force. Next, because φ_u is bounded so that parcels outside the storm are not moving in the same way as the inside parcels, the parcel deflection toward the southwest will induce a pile up of air in that quadrant of the storm creating a new geopotential which both balances the parcel motion toward the southeast and also, in a short time, will accelerate the parcels toward the northeast, beginning an inertia oscillation of the new basic current and geopotential balancing it in the northeast-southwest direction. The oscillation frequency will be near F and the period is of the order of six hours. The collection of parcels constituting the basic current are being continuously accelerated on the average toward the southeast by φ_u, and a new mean geopotential is being created to balance the new basic current. This new mean geopotential is the dashed lines in Fig. 9. Note that evidence of a current oscillation was given in Chapter V, and that the analyses of the wind and geopotential data give the mean or time average quantities.

Two points are to be noted concerning the southeastward parcel displacements. First, it would appear that southeast motion would destroy φ_u. No doubt φ_u may be diminished by this movement of mass along the gradient of φ_u, but as long as a net force is being exerted on the exterior of the storm, φ_u would exist. It is possible that the reduction of the acceleration rate of the storm with time may be related to net mass transport by the new basic current inside the storm. The second and most important note is that the average acceleration of the parcels toward the southeast must occur at a rate less than given by $\nabla\varphi_u$. There are two reasons; first, energy is lost from the mean current to gravity-inertia oscillations and, second, energy must be supplied to create the new mean geopotential which is denoted by φ_{geo} to indicate it is balanced geostrophically with the basic current. Since it is the rotation of the interior of the storm which causes the basic current acceleration to occur as described here, it is reasonable that the reduced rate of acceleration of the basic current as compared to $\nabla\varphi_u$ may be given by a simple non-dimensional parameter involving the rotation. The force controlling the current oscillation is proportional to F rather than f when no rotation of the fluid occurs; so it is proposed that the reduced storm and basic current acceleration rate is given by f/F.

The hypothesis of the basic current acceleration may be summarized in the following equations:

$$\dot{\bar{U}}_0 \cong - \frac{f}{F} \frac{\partial \varphi_u}{\partial x} , \qquad (6.37)$$

$$\dot{\bar{V}}_0 \cong - \frac{f}{F} \frac{\partial \varphi_u}{\partial y} , \qquad (6.38)$$

$$\bar{U}_0 = - \frac{1}{f} \frac{\partial \varphi_{geo}}{\partial y} , \qquad (6.39)$$

and

$$\bar{V}_0 = \frac{1}{f} \frac{\partial \varphi_{geo}}{\partial x} \qquad (6.40)$$

where the first pair of equations relate the basic current acceleration to φ_u and the second pair state the relation of the basic current to the new geopotential, φ_{geo}. The bar refers to time average conditions. According to the hypotheses, the storm acceleration and the time average basic current acceleration are equivalent so that the factor K in (6.1) and (6.2) should be given by

$$K = f/F. \qquad (6.41)$$

The hypotheses given above may be compared with the data for Betsy which were the motivation for them. First, the value of K may be computed from (6.41) and compared to the empirical value of K.

Values of F may be computed either from the observed symmetric wind or geopotential. Values of Z and Z_{gr} are found in Tables 7 and 14, respectively. Since these data vary with radius, it may be appropriate to compute an area weighted mean value. Area weighted values of K from (6.41) over a 125 km disk are K = .26 for the symmetric wind, and K = .22 for the symmetric geopotential. The latter value is adopted here and it compares favorably with the empirical value of K = .18 which makes (6.1) and (6.2) agree with observed mean acceleration of Betsy recorded between 1801 and 2110 GMT. Use of the average value of K seems appropriate even though the uniform geopotential gradient was obtained by giving primary weight to the data near 100 km, because this force is accelerating the whole storm inside 125 km and the higher rotation near the storm center should influence the acceleration. It may be noted in Fig. 8 that, if the uniform geopotential gradient is determined from data near 50 km, the unbalanced force in the x direction is doubled and the area average values of Z and Z_{gr} are also about doubled. The y profile of geopotential does not agree with this plan, but this may be the result of having the geopotential data missing on half of the north to south flight leg. The x geopotential profile is primarily the result of data collected along a southeast to northwest flight leg at about 1900 GMT. The average wind speed and thus the local value of Z is greater by about 5 m sec^{-1} in the west quadrant between 25 and 50 km than in the north or south quadrant, and this could influence the y profile also as compared to the x profile. It may be noted also that the asymmetric geopotential exists on the circumnavigation flight path at 2100 to 2200 GMT, which is after the storm acceleration has practically vanished, and φ_u must also exist beyond the time of the storm acceleration. This is possible because a net force acting in a thin layer in the middle of the storm need not cause an acceleration of the storm as forces at other levels may resist the acceleration, but when a storm is known to accelerate, it is most reasonable to find evidence of this fact at each level of the storm. This observation indicates that a complete picture of the storm acceleration is not obtained from a single data level and that forces may exist which have not been accounted for here.

The basic current acceleration hypothesized by (6.37) and (6.38) may be compared to the basic current in Table 5 by assuming that the observed mean values of U_0 and V_0 are created by φ_u between 1600 and 1930 GMT and that evidence of the U_0 and V_0 existing before 1600 GMT are lost in the adjustment process. The time 1930 GMT corresponds to the average time of the data collection, and 1600 GMT is assumed as the beginning of the acceleration. The results of computing the basic current for the given time interval and K = 0.22 are $U_0 = .79$ m sec^{-1} and $V_0 = -1.23$ m sec^{-1} at 125 km. At 100 km, the results are $U_0 = .64$ m sec^{-1} and $V_0 = -1.21$ m sec^{-1}; and, at 75 km, $U_0 = .69$ m sec^{-1} and $V_0 = -1.19$ m sec^{-1}. If the starting time is earlier than 1600 GMT, the values increase. The results above are in the right ballpark as compared with the non-divergent irrotational basic currents in Table 5. It is not entirely satisfactory to compute the basic current for 1930 GMT, as done here, without taking account of the fact that $\nabla\varphi_u$ may have been larger between 1600 and 1800 GMT than it was afterward, when our geopotential analysis was constructed. But, the change of storm speed was about 4 kt or 2 m sec^{-1} during the time 1600 to 1900 GMT, and this agrees with the basic current speed if the basic current is generated as assumed here. It is not reasonable to expect close agreement between the Table 5 data and the values computed here because, as pointed out in Chapter III, the observed basic current is influenced by vorticity and divergence distributions outside the disk where it is computed. The poorer verification at 125 km compared to 75 km may be related to this fact. It should also be noted that the hypotheses here may agree with the results of the wind acceleration computations of Chapter V, where it was found that the use of the observed mean U_0 and V_0 gave a good estimate of the equilibrium wind which may be interpreted to mean that $\dot{U}_0$ and $\dot{V}_0$ are small compared to $\nabla\varphi_u$.

Up to this point, a hypothesis of the acceleration of tropical storm Betsy has been given which reasonably agrees with the observed wind and geopotential data, but because the basic current computations in Table 5 do not agree with the movement of the storm, no explanation is apparent for the movement toward 330 degrees. The storm is moving far to the left of the basic currents defined by the average x and y components of the wind around a circle or defined by the non-divergent irrotational first harmonic wind over a disk or radius R. There is no apparent way to rationalize the movement of the storm with the basic current inside 125 km. The hypothesis presented here is that the movement of the storm toward 330 degrees is the result of movement of the storm vorticity field at 11,780 feet by the observed wind field rather than by the first harmonic of the wind, as use of the basic current to explain the movement implies. Examination of the isotach field of Fig.

5 gives the basis for this hypothesis. Here, it is shown that the wind speed on the right side of the storm looking toward the direction of motion is consistently greater than on the left side and in the range of 75 to 125 km, the difference in speed between the right and left side is about 10 kts. This compares favorably with the observed speed of the storm which varies from 12 to 6 kt during the flight.

The view of the storm movement inside 125 km given here may be the result of vertical momentum transfer in cumulus convection in the storm core. Vertical momentum transfer in cumulus clouds, which have a time scale of half an hour and a horizontal scale of a few kilometers, is probably responsible for keeping the storm moving at the same velocity at each level, so it is reasonable that the higher wind harmonics play an important role in the storm movement. It should also be noted that vertical momentum transfer may result in a net force upon the air at one level and that the right distribution of such forces can induce acceleration of the storm as viewed from this level, as well as local wind accelerations. Such a force is a three-dimensional problem and has not been considered in the discussion of Betsy from data at 11,780 feet. This force need not be important in each case of storm acceleration for, if a force acting on the outer part of the storm is nearly uniform for a deep layer, little internal adjustment may be required.

CHAPTER VII

SUMMARY OF RESULTS

The objective of this study has been to examine the acceleration of the hurricane through data collected both inside and outside the storm. The difficulties of doing this were apparent in the discussion of those data in Chapters III and VI. Time compositing of the aircraft reconnaissance data and scarcity of synoptic data were the major data problems.

Examination of the acceleration and motion of Betsy revealed significant differences between the inside and outside of the storm. First, the distinction between the inside and outside is that the basic current disagrees and agrees, respectively, with the environment steering current in these areas. The boundary between inside and outside could not be observed in these data, even though this region may be critical in understanding the storm acceleration.

If only data outside the storm is used, the storm motion and acceleration agree reasonably well with the theory of Kuo, who included drag forces to explain the deviation of the motion from the steering current, and when steering current acceleration is added to the model, some agreement is obtained between the observed storm acceleration and the theory. In particular, the movement and acceleration vectors of the storm are near 30 degrees to the right of the steering current and its acceleration. Data were so poor, however, that the results are tentative.

The picture inside the storm is quite different from that outside. An unbalanced uniform geopotential gradient force was found which is colinear with the observed storm acceleration but about five times greater in magnitude. It was hypothesized that this force was the reflection inside the storm of the storm-environment interaction predicted by Kuo's theory. The unbalanced geopotential force is of the same order as the expected wind acceleration in Betsy, excluding the convection region, as discussed in Chapter V. To relate this force to the storm acceleration, it was hypothesized that a mean air-parcel acceleration occurs down the geopotential gradient through an adjustment mechanism controlled by the storm rotation in such a manner that the mean acceleration, which was identified with the basic current acceleration, is of the order of the observed hurricane acceleration while the instantaneous acceleration of air parcels, including gravity-inertia oscillations, may agree with the unbalanced force. Since rotation controls the adjustment mechanism, the parameter f/F was proposed to relate the unbalanced force to the storm and basic current acceleration. The hypotheses are supported by agreement between the observed $f/F = .22$ and the empirical value of .18, the direction and magnitude of the basic current at 287° 2.7 kts, and the observation of an inertia oscillation in the wind field whose period is near six hours.

It may be interesting to note the analogy between our hypotheses for the acceleration of Betsy inside 125 km and the approach of Sasaki and Syono. They filtered the high frequency oscillation from the storm acceleration by introducing a parameter ϵ, which is essentially f/Z. We have filtered the gravity-inertia oscillations from the mean acceleration of air parcels down the unbalanced geopotential gradient and the storm acceleration by introducing f/F.

The direction of the basic current inside 125 km agrees with the acceleration hypothesis but does not help explain the movement of the storm in nearly the opposite direction. It was hypothesized that the storm motion is the result of movement of the storm vorticity field by the observed wind field, rather than just by the basic current. This concept was not tested by computation and will be, but the isotach data agree with the idea, showing stronger winds on the right side of the storm than on the left.

An important calculation of the observed wind acceleration was reported in Chapter V. The calculations showed the approach of the wind field toward approximate equilibrium with the symmetric geopotential and showed the dominance of the symmetric over the non-symmetric geopotential. In particular, the acceleration of the basic current appeared to be much smaller than the geopotential data suggested. It was these observations which ultimately lead to the hypothesis of storm acceleration inside 125 km.

It must be understood that the discussion of hurricane motion given here was derived from one level of data and two-dimensional theories. Further investigation of three-dimensional structure may reveal important concepts not included here. In particular, aircraft data of the wind field exist at 1770 feet on this day for Betsy and show a basic current inside 125 km which may agree with the motion of the storm. Geopotential data were not available.

BIBLIOGRAPHY

Cahn, A., 1945: An investigation of free oscillations of a simple current system. J. Meteor., 2, 113-119.

Charney, J., 1948: On the scale of atmospheric motions. Geofys. Publikasjoner, 17, 2, 17 pp.

__________, 1949: On a physical basis for numerical prediction of large-scale motions in the atmosphere. J. Meteor., 6, 371-385.

Kuo, H. L., 1969: Motions of vortices and circulating cylinder in shear flow with friction. J. Atmos. Sci., 26, 390-398.

Riehl, H., 1954: Tropical Meteorology. New York, McGraw Hill, 392 pp.

Rossby, C. G., 1938: On the mutual adjustment of pressure and velocity distribution in certain simple current systems, II. J. of Mar. Res., 1, 239-263.

Sasaki, Y., 1958: An objective analysis based on the variational method. J. Meteor. Soc. Japan, 36, 77-88.

Sasaki, Y. and K. Miyakoda, 1954: Numerical forecasting of the movement of cyclones. J. Meteor. Soc. Japan, 32, 325-335.

Sasaki, Y. and S. Syono, 1966: Motion of a vortex with pressure and inflow which are not circular symmetry. Univ. of Oklahoma Research Institute, ARL-1470-3. 64 pp.

__________, 1968: Motion of tropical cyclones. Unpublished manuscript. Dept. of Meteorology, University of Oklahoma. 30 pp.

Syono, S., 1955: On the motion of a typhoon (I). J. Meteor. Soc. Japan, 33, 245-261.

Yeh, Tu-cheng, 1950: The motion of tropical storms under the influence of a superimposed southerly current. J. Meteor., 7, 108-113.

TABLE 1

TRACK DATA FOR BETSY ON 29 AUGUST 1965

Time Interval	Velocity degree/kt	$\dot{X}$ m sec^{-1}	$\dot{Y}$ m sec^{-1}
1537 - 1555	327/12	- 3.36	5.18
1555 - 1601	326/12	- 3.45	5.12
1601 - 1624	326/11	- 3.17	4.69
1624 - 1637	325/11	- 3.25	4.64
1637 - 1715	325/10	- 2.95	4.22
1715 - 1718	325/9	- 2.66	3.80
1718 - 1801	326/9	- 2.59	3.84
1801 - 1832	326/8	- 2.30	3.41
1832 - 1900	327/8	- 2.24	3.45
1900 - 1903	328/8	- 2.18	3.49
1903 - 1926	328/7	- 1.91	3.06
1926 - 2005	329/7	- 1.86	3.09
2005 - 2047	330/7	- 1.80	3.12
2047 - 2110	331/7	- 1.75	3.15
2110 - 2133	331/6	- 1.50	2.70
2133 - 2241	332/6	- 1.45	2.73
2241 - 2310	333/6	- 1.40	2.75
2310 - 2358	334/6	- 1.35	2.78

TABLE 2

MEAN ACCELERATION OF BETSY ON 29 AUGUST 1965

Time Interval	$\bar{\ddot{X}} \times 10^{-4} m\ sec^{-2}$	$\bar{\ddot{Y}} \times 10^{-4} m\ sec^{-2}$
1601 - 1637	1.20	- 2.08
1637 - 1715	1.14	- 1.97
1715 - 1801	0.94	- 1.63
1801 - 1903	0.70	- 1.21
1903 - 2110	0.34	- 0.59
1801 - 2110	0.46	- 0.79
1601 - 2110	0.69	- 1.21

TABLE 3

FIRST HARMONIC OF GEOPOTENTIAL AND WIND

Radius	φ_1	φ_1^*	V_{r1}	V_{r1}^*	$V_{\theta 1}$	$V_{\theta 1}^*$
km	$m^2 sec^{-2}$	$m^2 sec^{-2}$	$m\ sec^{-1}$	$m\ sec^{-1}$	$m\ sec^{-1}$	$m\ sec^{-1}$
12.5	- 4.93	20.74	4.74	- 4.87	- 4.78	- 3.31
25.	-23.22	9.51	5.77	- 5.58	- 6.04	- 2.74
37.5	-25.30	7.19	6.33	- 5.96	- 5.36	0.96
50.	-48.10	16.72	6.41	- 5.45	- 4.21	0.52
62.5	-38.52	22.50	5.86	- 5.59	- 4.43	- 0.61
75.	-40.57	31.92	5.56	- 5.51	- 4.20	- 2.04
87.5	-37.98	38.44	5.36	- 5.65	- 3.22	- 2.54
100.	-37.77	41.68	5.02	- 5.73	- 1.86	- 2.29
112.5	-34.31	44.00	4.69	- 5.92	- 1.52	- 2.39
125.	-43.67	47.57	4.35	- 5.68	- 2.06	- 3.36

TABLE 4

SECOND HARMONIC OF GEOPOTENTIAL AND WIND

Radius	φ_2	φ_2^*	$V_{r\,2}$	$V_{r\,2}^*$	$V_{\theta\,2}$	$V_{\theta\,2}^*$
km	$m^2 sec^{-2}$	$m^2 sec^{-2}$	$m\ sec^{-1}$	$m\ sec^{-1}$	$m\ sec^{-1}$	$m\ sec^{-1}$
12.5	- 5.27	6.29	0.28	0.84	- 0.02	0.29
25.	-23.78	14.15	0.47	1.29	0.08	0.53
37.5	-30.00	9.34	1.51	1.24	0.37	0.71
50.	-41.79	8.18	1.57	1.25	1.65	1.53
62.5	-32.17	-2.28	1.16	0.76	1.47	0.68
75.	-34.76	-3.31	0.69	0.41	1.27	-0.22
87.5	-27.55	-1.36	0.47	0.18	1.23	-0.20
100.	-18.91	-0.12	0.48	-0.07	0.79	0.26
112.5	-11.24	-3.19	0.34	-0.04	0.22	0.55
125.	- 5.82	-5.47	0.18	-0.04	-0.06	0.32

TABLE 5

BASIC CURRENT COMPUTATION

Radius	(3.1)	(3.2)	non-divergent,	irrotational
	U_0	V_0	U_0	V_0
km	m sec^{-1}	m sec^{-1}	m sec^{-1}	m sec^{-1}
0.	-	-	1.71	- 0.80
12.5	1.72	- 0.82	1.64	- 1.01
25.	1.94	- 1.54	1.49	- 1.17
37.5	0.37	- 1.65	1.32	- 1.27
50.	0.64	- 0.82	1.17	- 1.30
62.5	0.92	- 1.00	1.08	- 1.25
75.	1.49	- 0.84	1.06	- 1.13
87.5	1.64	- 0.42	1.09	- 0.96
100.	1.34	.0.22	1.18	- 0.76
112.5	1.23	0.28	1.27	- 0.56
125.	1.54	0.14	1.32	- 0.40

TABLE 6

FIRST HARMONIC WIND-QUARTIC POLYNOMIAL

Radius km	V_{r1} m sec^{-1}	V_{r1}^* m sec^{-1}	$V_{\theta 1}$ m sec^{-1}	$V_{\theta 1}^*$ m sec^{-1}
0.	4.03	- 4.82	- 4.82	- 4.03
12.5	5.07	- 5.08	- 5.13	- 2.70
25.	5.76	- 5.28	- 5.33	- 1.49
37.5	6.12	- 5.43	- 5.31	- 0.63
50.	6.20	- 5.54	- 5.02	- 0.27
62.5	6.05	- 5.61	- 4.47	- 0.42
75.	5.75	- 5.66	- 3.72	- 1.03
87.5	5.35	- 5.69	- 2.89	- 1.91
100.	4.94	- 5.71	- 2.15	- 2.78
112.5	4.60	- 5.73	- 1.73	- 3.26
125.	4.42	- 5.77	- 1.92	- 2.86

TABLE 7

SYMMETRIC WIND, $v_{\theta 0}$, MEAN ANGULAR SPEED, Z, AND

DOUBLET COMPONENTS D AND D*

Radius	$v_{\theta 0}$	Z	D	D^*
km	m sec^{-1}	$10^{-4} sec^{-1}$	m sec^{-1}	m sec^{-1}
12.5	9.78	7.82	0.72	-0.04
25.	13.13	5.25	1.52	0.49
37.5	14.54	3.88	3.64	-0.30
50.	13.42	2.68	3.46	-0.62
62.5	12.29	1.97	2.62	-0.58
75.	11.65	1.55	1.76	-0.66
87.5	11.60	1.33	1.41	-1.22
100.	12.22	1.22	1.36	-1.93
112.5	12.11	1.08	1.15	-2.20
125.	11.12	0.89	0.50	-1.81

Area weighted average of Z = 1.86

TABLE 8

BALANCE OF WIND AND φ_1/R IN UNIT OF 10^{-4}m sec^{-2}

R	φ_1/R	fV_0	$Z(D^* - \delta V)$		fD^*
km			9KT	6KT	
12.5	- 3.92	- 0.50	37.77	28.95	- 0.02
25.	- 9.28	- 0.59	30.90	23.61	0.25
37.5	- 6.75	- 0.64	18.97	13.87	- 0.15
50.	- 9.65	- 0.65	12.62	9.03	- 0.31
62.5	- 6.16	- 0.63	9.23	6.68	- 0.29
75.	- 5.41	- 0.57	6.91	4.85	- 0.33
87.5	- 4.34	- 0.48	5.01	3.23	- 0.61
100.	- 3.77	- 0.38	3.41	1.79	- 0.97
112.5	- 3.05	- 0.28	2.58	1.12	- 1.10
125.	- 3.50	- 0.21	2.31	1.13	- 0.91

TABLE 9

BALANCE OF WIND AND φ_1^*/R IN UNIT OF 10^{-4}m $\sec^{-2}$

R	φ_1^*/R	$-fU_0$	$Z(\delta U - D)$		$-fD$
km			9KT	6KT	
12.5	16.56	- 0.82	24.40	18.46	- 0.36
25.	3.80	- 0.75	12.57	8.32	- 0.76
37.5	1.92	- 0.66	-0.04	-3.01	- 1.82
50.	3.34	- 0.59	0.11	-1.98	- 1.73
62.5	3.60	- 0.54	1.47	-0.06	- 1.31
75.	4.25	- 0.53	2.51	1.31	- 0.88
87.5	4.38	- 0.55	2.61	1.57	- 0.71
100.	4.17	- 0.59	2.60	1.66	- 0.68
112.5	3.91	- 0.64	2.66	1.81	- 0.58
125.	3.80	- 0.66	2.76	2.08	- 0.25

TABLE 10

ACCELERATION FROM (4.4) AND (4.6) IN UNIT OF 10^{-4}m sec^{-2}

Radius km	$\dot{U}_0$	$\dot{D}$ 9KT	$\dot{D}$ 6KT
12.5	2.25	- 38.62	- 29.80
25.	2.46	- 37.38	- 30.09
37.5	2.41	- 22.52	- 17.42
50.	2.40	- 18.91	- 15.32
62.5	2.42	- 12.05	- 9.50
75.	2.48	- 8.94	- 6.88
87.5	2.57	- 5.69	- 3.91
100.	2.67	- 3.16	- 1.54
112.5	2.77	- 1.48	- 0.02
125.	2.84	- 1.85	- 0.67

TABLE 11

ACCELERATION FROM (4.5) AND (4.7) IN UNIT OF 10^{-4}m sec^{-2}

Radius	$\dot{V}_0$	$\dot{D}^*$	
km		9KT	6KT
12.5	- 4.62	- 11.28	- 5.34
25.	- 4.55	- 11.81	- 7.56
37.5	- 4.46	- 0.02	2.95
50.	- 4.39	1.16	3.25
62.5	- 4.34	- 0.36	1.17
75.	- 4.33	- 1.18	0.02
87.5	- 4.35	- 1.32	- 0.28
100.	- 4.39	- 1.55	- 0.61
112.5	- 4.44	- 1.97	- 1.12
125.	- 4.46	- 2.51	- 1.83

TABLE 12

WIND OBSERVATION PARIS IN MOVING COORDINATE

Point number	Azmuth degree	Radius km	Time GMT	Δt hr	First Wind Obs. degree kts	Second Wind Obs. degree kts
1	030	115	1736	4.30	159.6/26.3	153.2/41.4
2	055	105	1742	4.33	128.6/27.3	128.6/28.6
3	097.5	87.5	1758	4.2	065.3/22.2	062.3/23.8
4	100	60	1803	4.95	008.3/21.3	064.5/24.2
5	150	45	1921	3.75	001.0/22.3	010.9/32.2
6	150	100	1929	2.95	003.0/20.1	026.0/30.5
7	172.5	27.5	2016	0.4	008.0/22.8	327.9/42.8
8	173	87.5	2049	1.7	350.5/26.5	007.3/31.3
9	185	60	2237	0.55	359.0/33.1	347.8/40.3
10	190	45	2012	2.45	327.5/31.6	007.0/30.2
11	200	75	2007	3.1	310.8/31.25	342.5/34.25
12	202.5	90	2005	3.2	314.0/18.3	345.6/26.60
13	205	105	2003	3.25	324.6/21.0	347.4/24.4
14	205	120	2000	3.33	320.0/17.3	328.6/27.3
14a	205	120	2000	0.96	320.0/17.3	316.9/21.7
15	270	115	1826	2.85	278.6/25.2	277.4/28.8
16	290	125	1835	2.8	249.2/22.1	269.8/25.4
17	305	125	1634	2.1	237.9/20.1	234.9/27.8
18	325	125	1845	2.85	212.8/28.9	218.4/25.6
19	330	120	1847	2.85	210.0/32.8	207.0/22.9

TABLE 13

OBSERVED WIND AND ACCELERATION COMPONENTS

Point number	First Wind Obs. ($m\ sec^{-1}$)		Second Wind Obs. ($m\ sec^{-1}$)		Average Acceleration ($10^{-4} m\ sec^{-2}$)	
	$u+\dot{X}$	$v+\dot{Y}$	$u+\dot{X}$	$v+\dot{Y}$	$\dot{u}+\ddot{X}$	$\dot{v}+\ddot{Y}$
1	- 4.72	12.96	- 9.61	19.02	- 3.16	4.09
2	-10.96	8.75	-11.51	9.18	- 0.35	- 0.28
3	-10.38	- 4.78	-10.84	- 5.70	- 0.30	- 0.61
4	- 1.58	-10.85	-11.24	- 5.36	- 5.42	3.08
5	- 0.20	-11.47	- 3.13	- 16.27	- 2.47	- 3.55
6	- 0.52	-10.00	- 6.88	- 14.11	- 5.99	- 3.87
7	- 1.64	-11.66	11.69	- 18.64	92.54	-48.47
8	2.25	-13.45	- 2.03	- 15.98	- 6.99	- 4.13
9	0.01	-17.04	4.40	- 20.27	22.17	-16.39
10	8.74	-13.72	- 1.89	- 15.43	-12.05	- 1.94
11	12.18	-10.51	5.30	- 16.81	- 6.16	- 5.64
12	6.78	- 6.53	3.40	- 13.22	- 2.93	- 5.80
13	6.23	- 8.83	2.78	- 12.25	- 2.95	- 2.92
14	5.72	- 6.82	7.32	- 11.99	1.33	- 4.31
14a	5.72	- 6.82	7.64	- 8.17	5.44	- 3.84
15	12.82	- 1.94	14.70	- 1.91	1.83	0.03
16	10.64	4.04	12.86	2.33	2.21	- 1.70
17	8.77	5.50	11.68	8.21	3.85	3.59
18	8.05	12.51	8.18	10.33	0.13	- 2.12
19	8.43	14.60	5.35	10.50	- 3.00	- 4.00

TABLE 14

SYMMETRIC GEOPOTENTIAL, φ_0, GRADIENT WIND, $v_{\theta\ gr}$,

AND ANGULAR SPEED OF GRADIENT WIND, Z_{gr}

Radius km	φ_0 m^2sec^{-2}	$v_{\theta\ gr}$ $m\ sec^{-1}$	Z_{gr} $10^{-4}sec^{-1}$
12.5	891.38	-	-
25.	982.61	12.43	4.97
37.5	1061.50	14.82	3.95
50.	1147.60	15.67	3.13
62.5	1204.00	15.33	2.45
75.	1260.80	15.20	2.03
87.5	1300.10	14.51	1.66
100.	1339.10	15.22	1.52
112.5	1377.00	16.07	1.43
125.	1416.60	17.02	1.36

Area Weighted Average of Z_{gr} = 1.76

TABLE 15

EQUILIBRIUM WIND OF (5.36) AND (5.37) AND u_{gr}, v_{gr}, u_{geo}, v_{geo}

Point number	$u + \dot{X}$ m sec^{-1}	$v + \dot{Y}$ m sec^{-1}	u_{gr} m sec^{-1}	v_{gr} m sec^{-1}	u_{geo} m sec^{-1}	v_{geo} m sec^{-1}
1	- 8.99	11.70	- 8.13	14.07	- 6.96	- 7.94
2	-13.92	6.87	-12.61	8.83	- 8.96	- 6.54
3	-14.85	- 4.13	-14.37	- 1.89	- 6.40	- 8.36
4	-15.52	- 5.60	-15.17	- 2.93	- 8.82	-14.34
5	- 6.02	-13.66	- 6.45	-11.17	- 5.48	-16.68
6	- 7.33	-12.99	- 7.61	-13.18	- 2.82	2.00
7	- 1.17	-14.62	- 1.68	-12.79	- 6.94	-15.22
8	- 2.49	-14.62	- 1.77	-14.39	- 7.44	2.18
9	0.99	-14.66	1.26	-14.44	- 8.34	0.68
10	2.87	-16.38	2.52	-14.28	- 6.12	-13.66
11	3.75	-14.52	5.20	-14.29	-12.62	0.47
12	3.81	-13.80	5.62	-13.58	-11.96	0.37
13	4.97	-15.04	6.55	-14.05	-10.10	- 2.72
14	6.46	-17.26	7.02	-14.04	- 5.68	-11.02
15	15.93	- 2.79	16.25	- 0.85	- 4.90	- 5.45
16	14.64	3.55	15.97	5.81	- 8.50	- 7.32
17	12.16	7.11	13.92	9.75	-10.08	- 8.72
18	7.81	10.55	9.75	13.92	-10.74	-11.44
19	6.94	11.81	8.35	14.46	- 8.96	- 8.90

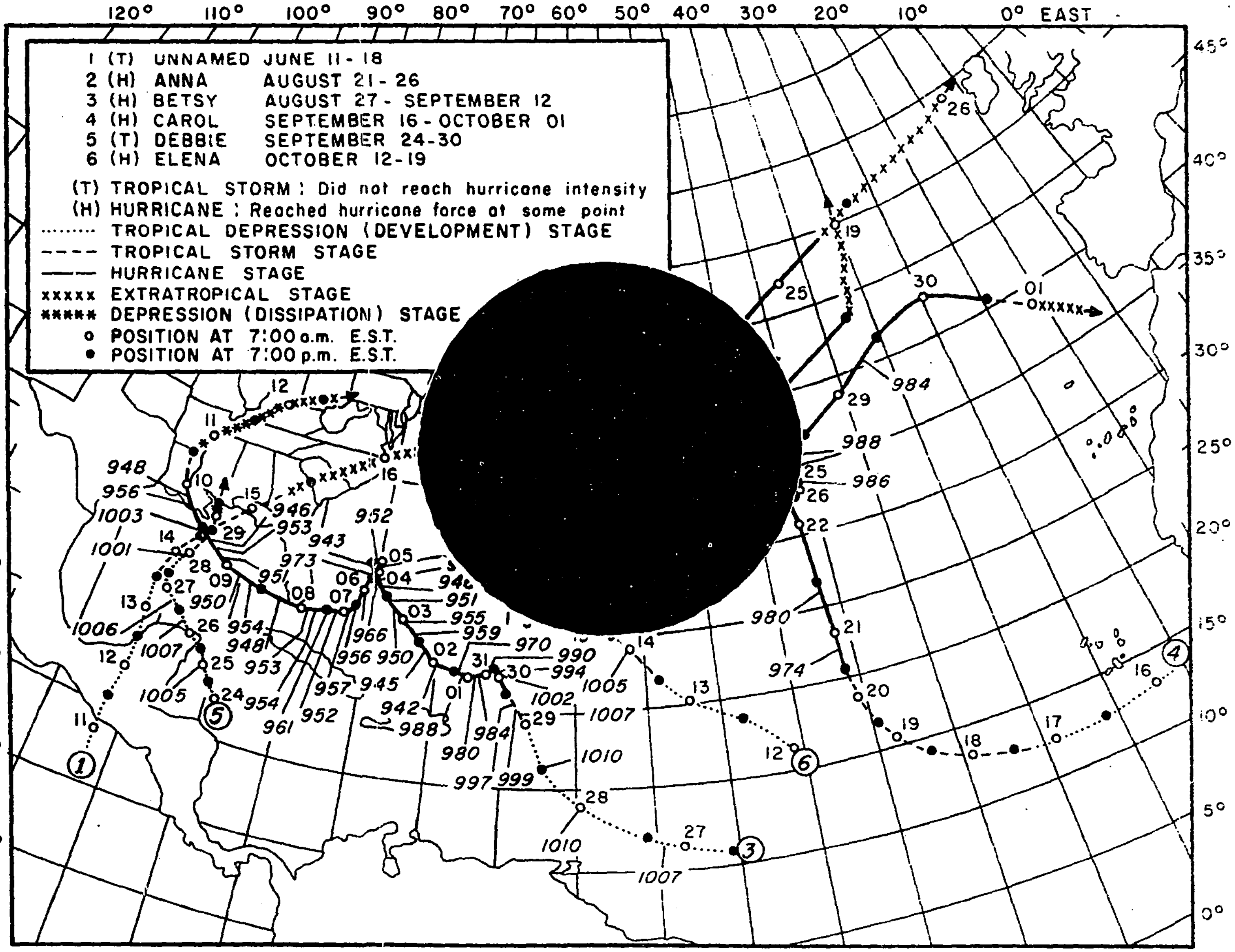

Fig. 1. Storm tracks of 1965.

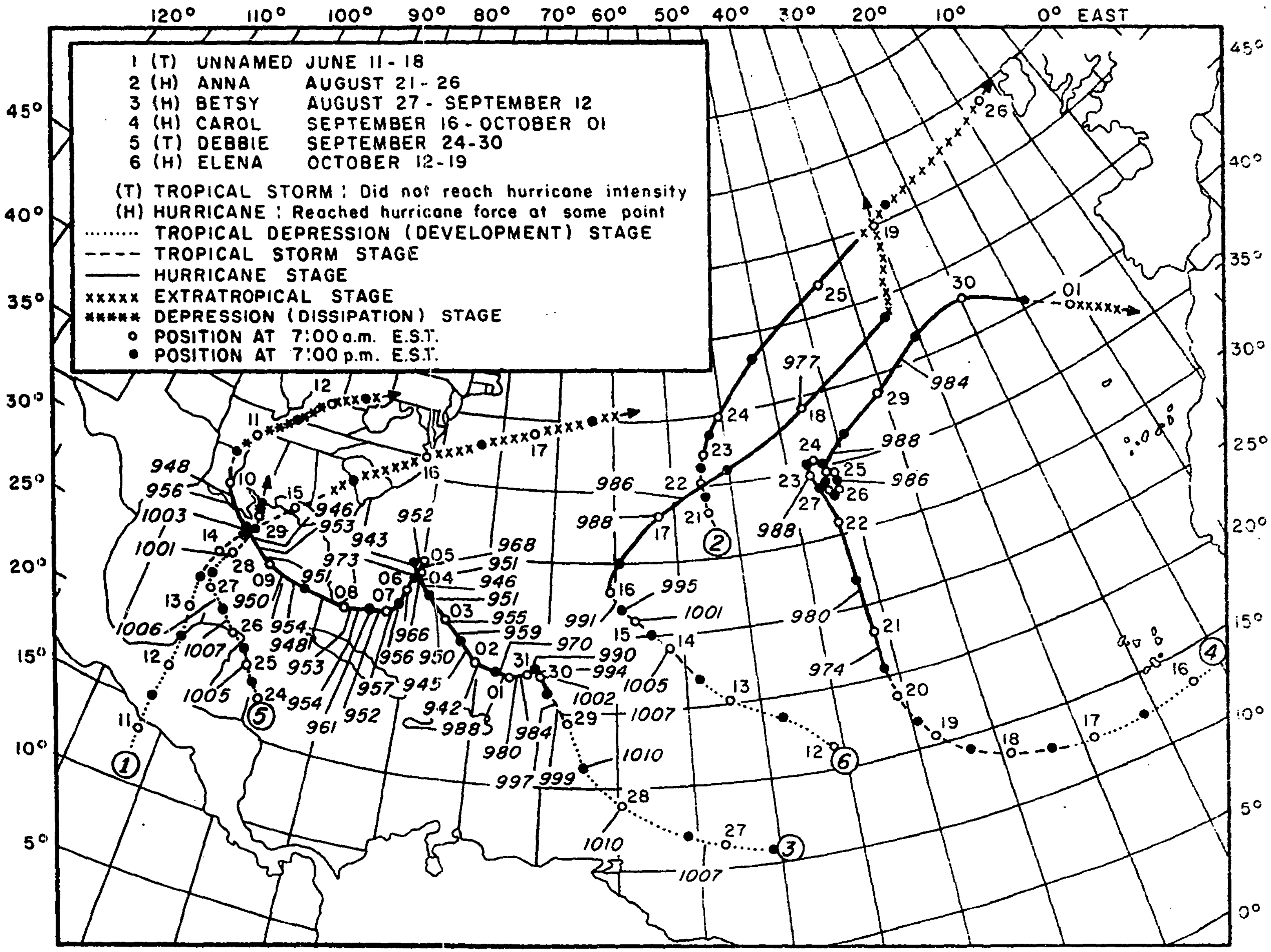

Fig. 1. Storm tracks of 1965.

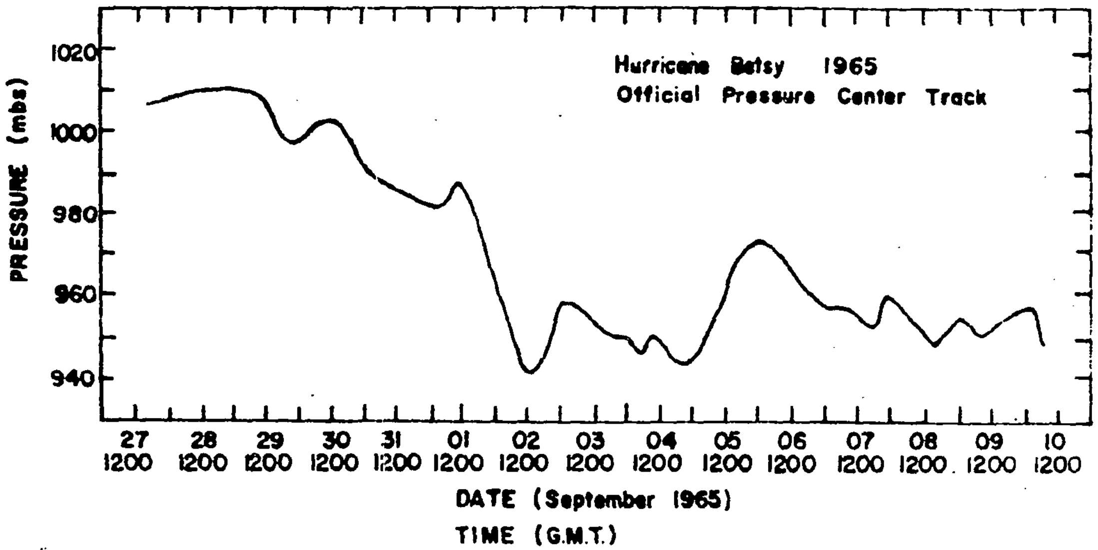

Fig. 2. Betsy central pressure trace.

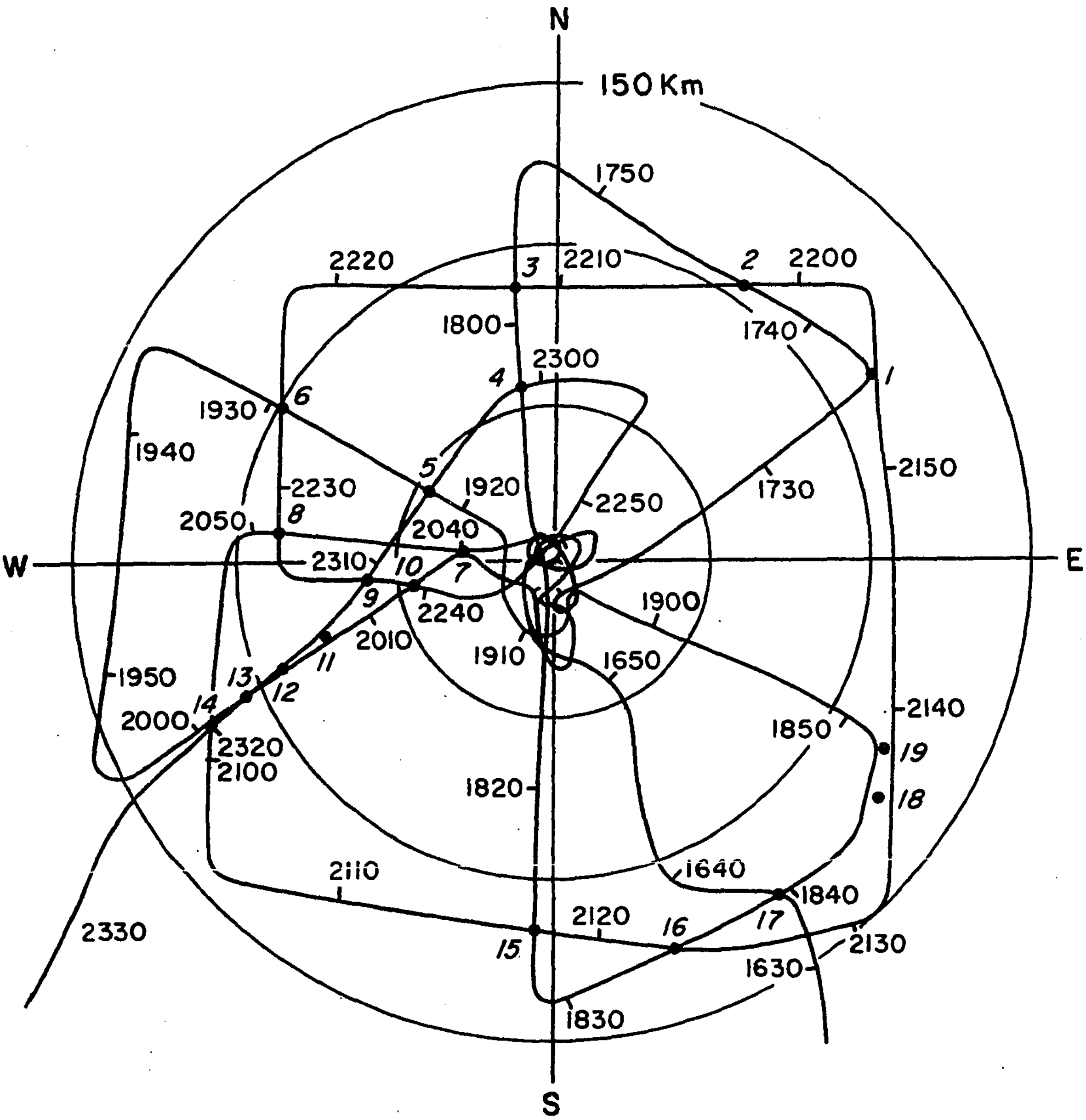

Fig. 3. Flight path at 11,780 ft in Betsy, 29 August 1965, shown with respect to moving storm center. Time along path is GMT. Wind acceleration points are numbered 1-19.

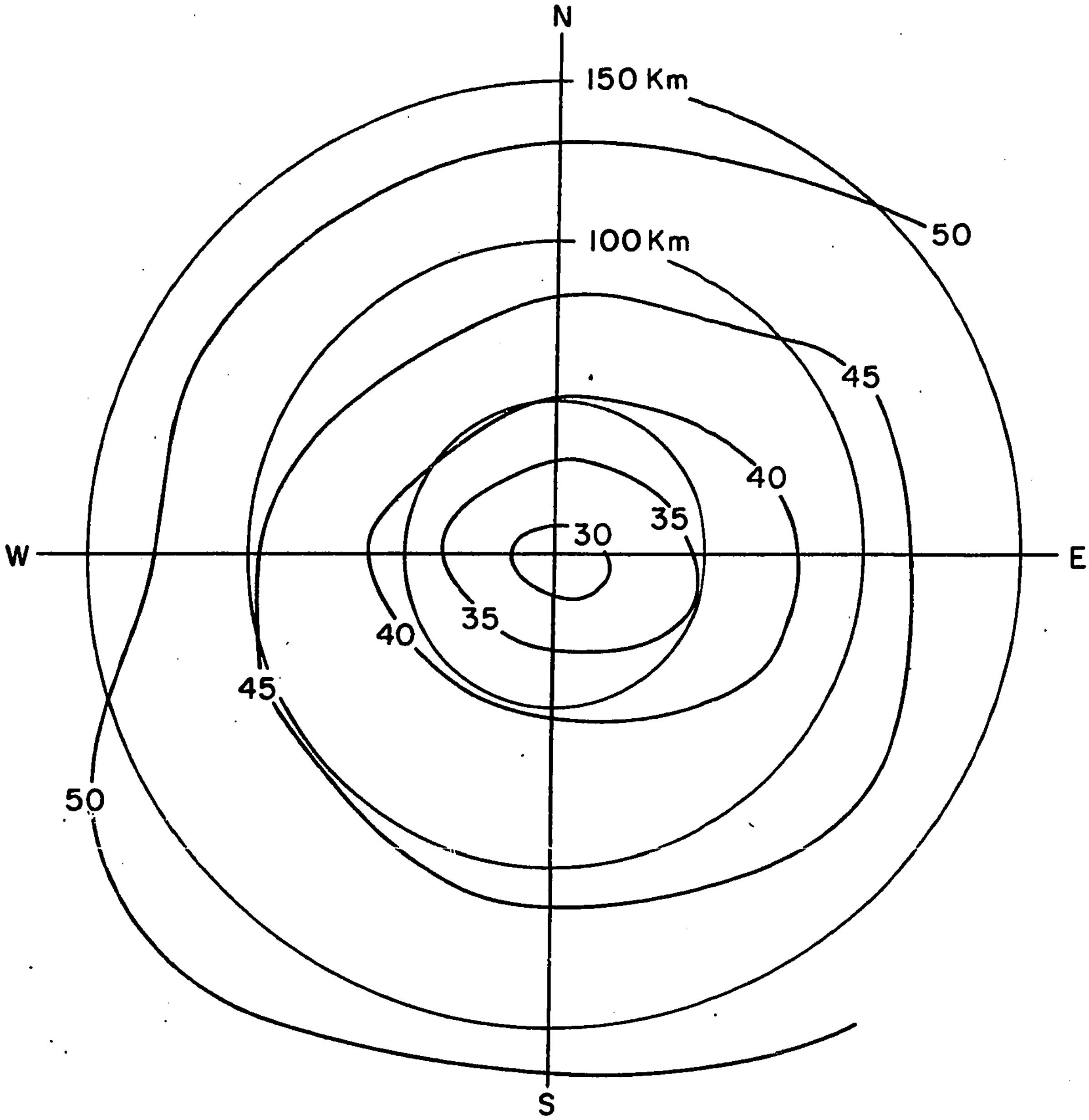

Fig. 4. D-value analysis in decafeet.

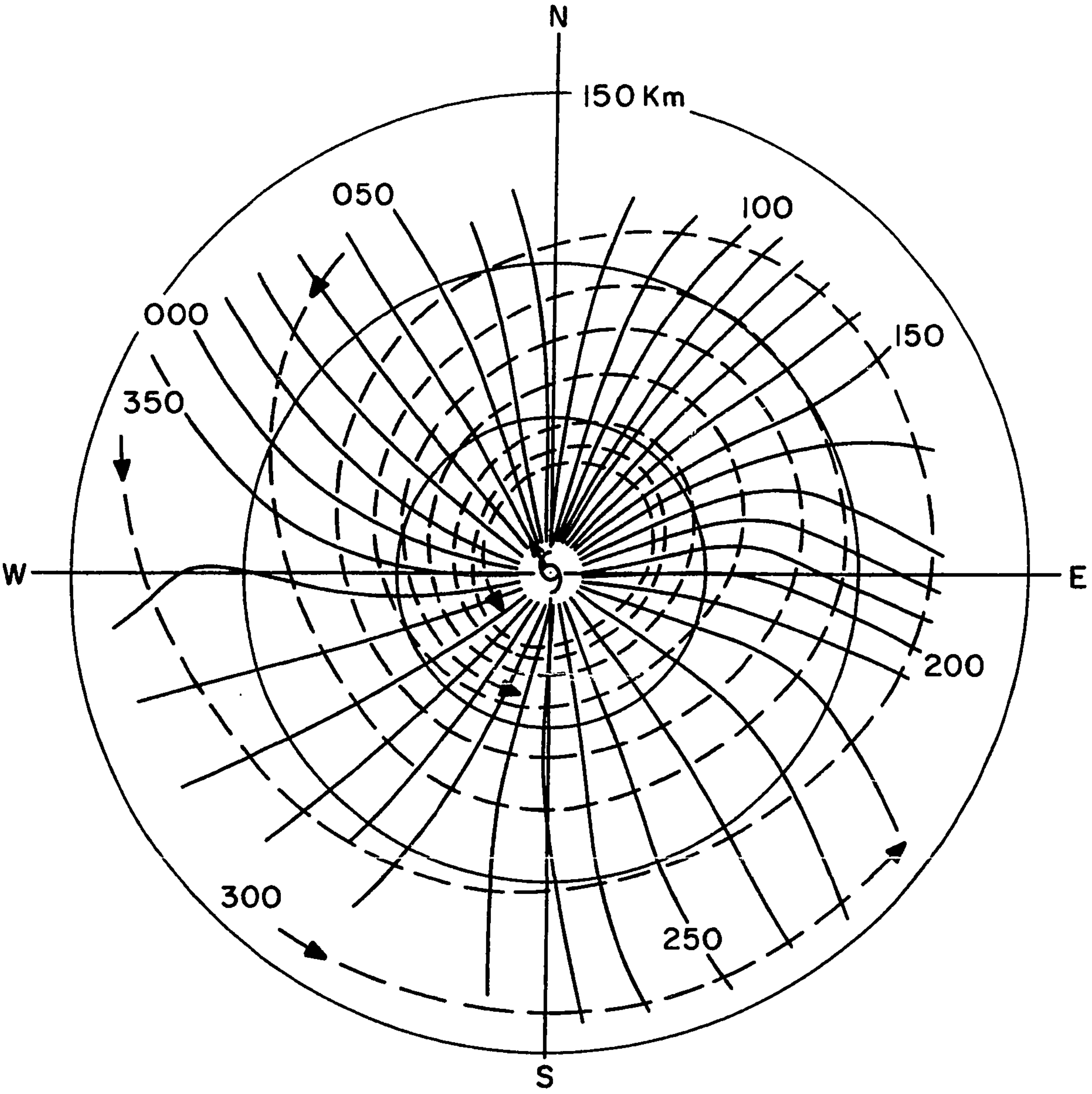

Fig. 5: Streamline and isogon analysis with north wind 000 east 090 etc.

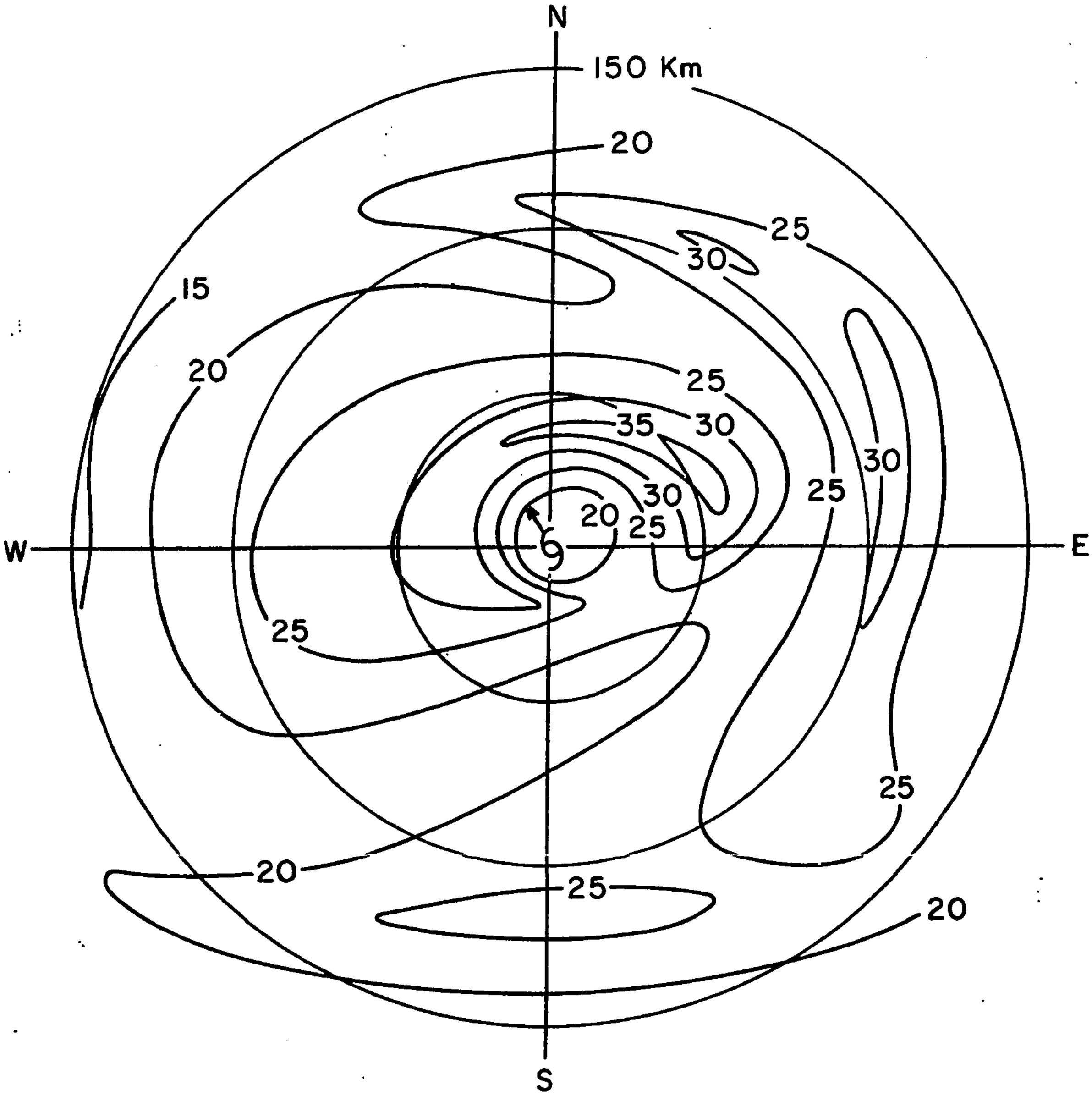

Fig. 6. Isotach analysis unit is knot. Storm motion denoted by arrow at center.

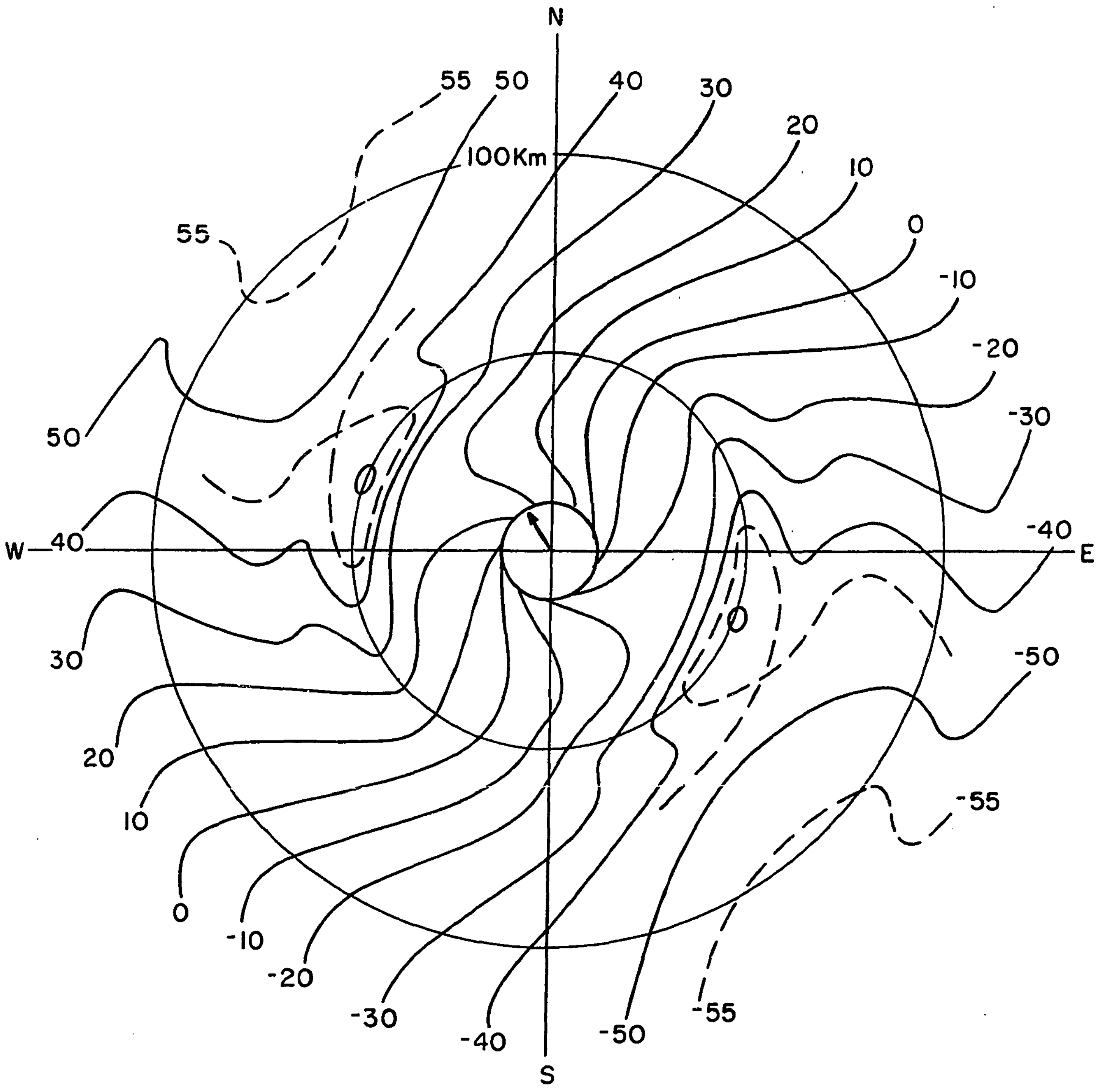

Fig. 7. First harmonic of geopotential in $m^2 sec^{-2}$.

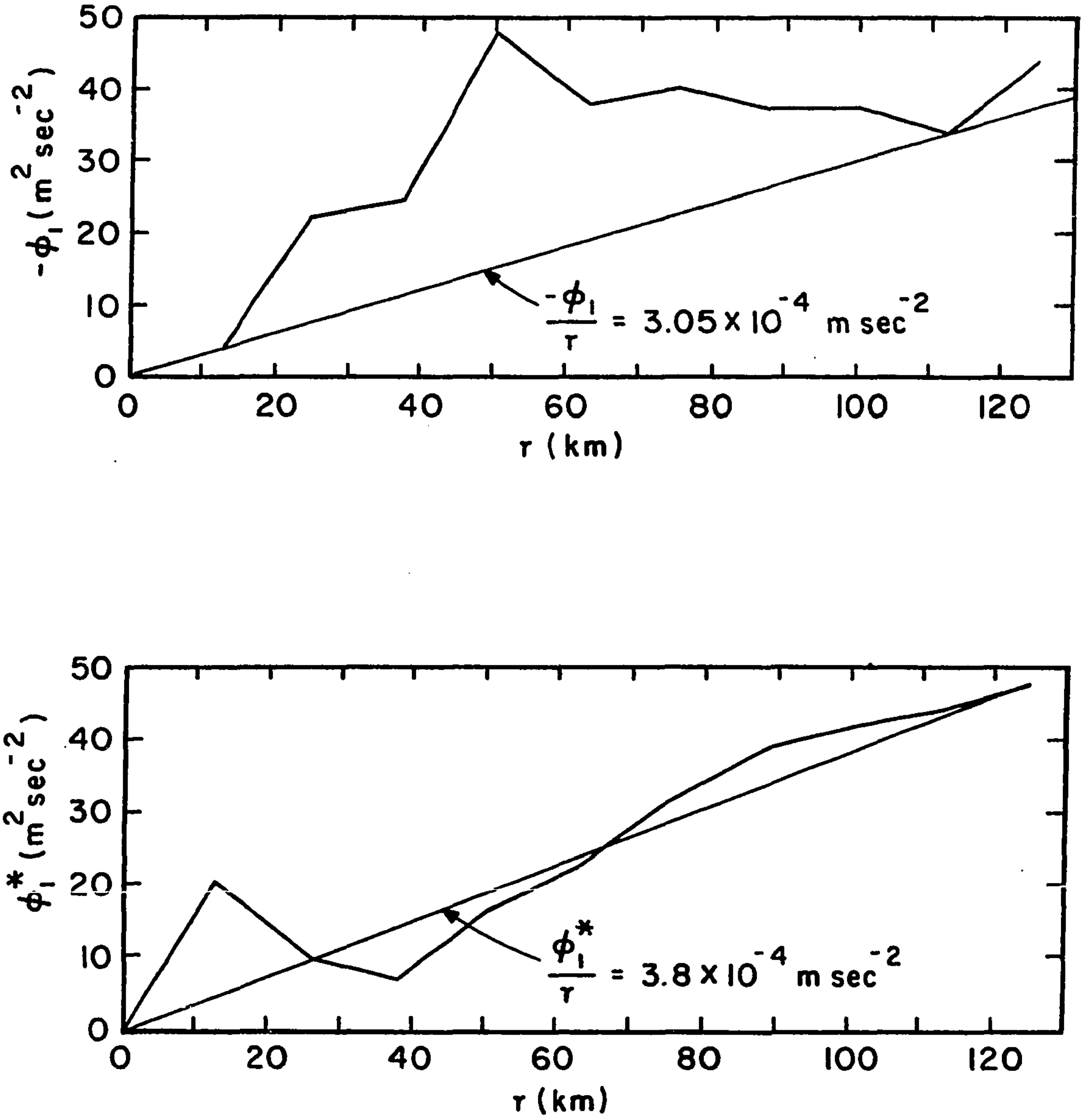

Fig. 8. Radial profiles of φ_1 and φ_1^*.

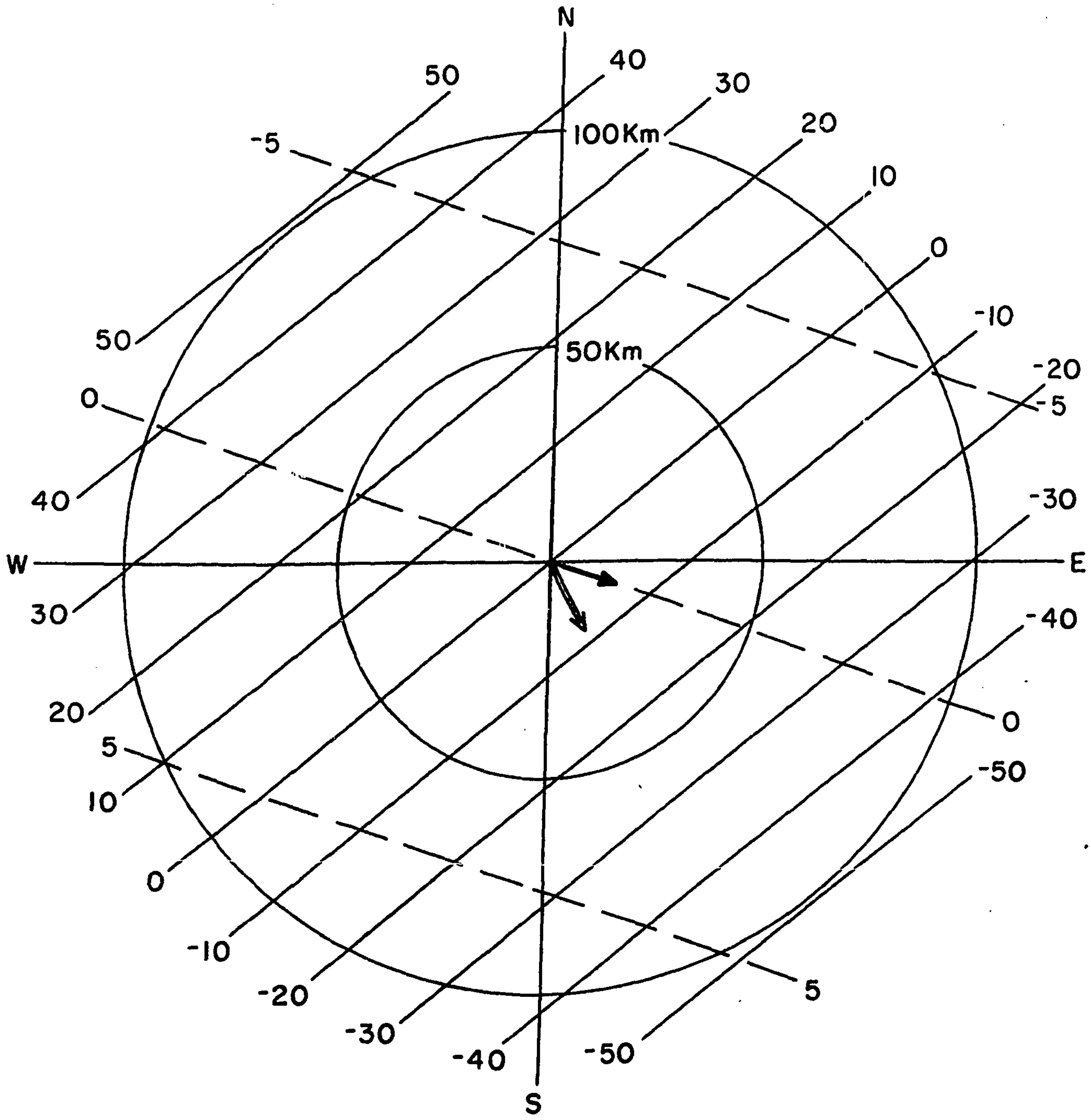

Fig. 9. Uniform gradient of the first harmonic of geopotential in $m^2 sec^{-2}$. Basic current at 125 km denoted by solid arrow and mean storm acceleration by open arrow. Dashed lines are geopotential balanced by basic current at 125 km.